STRUCTURAL EVALUATION OF SLAB REHABILITATION BY METHOD OF HYDRODEMOLITION AND LATEX MODIFIED OVERLYAY

by

Matthew Jeffrey McCabe

Bachelor of Science in Civil Engineering, University of Pittsburgh, 2011

Submitted to the Graduate Faculty of

The Swanson School of Engineering in partial fulfillment

of the requirements for the degree of

Master of Science in Civil Engineering

University of Pittsburgh

2013

UNIVERSITY OF PITTSBURGH

SWANSON SCHOOL OF ENGINEERING

This thesis was presented

by

Matthew Jeffrey McCabe

It was defended on

September 4, 2013

and approved by

John Brigham, Ph.D., Assistant Professor, Dept. of Civil and Environmental Engineering

Qiang Yu, Ph.D., Assistant Professor, Dept. of Civil and Environmental Engineering

Thesis Advisor:

Kent A. Harries, Ph. D., Associate Professor, Dept. of Civil and Environmental Engineering

STRUCTURAL EVALUATION OF SLAB REHABILITATION BY METHOD OF HYDRODEMOLITION AND LATEX MODIFIED OVERLYAY

Matthew J. McCabe

University of Pittsburgh, 2013

The objective of this work was to verify whether reinforced concrete bridge deck slabs repaired by means of hydrodemolition (HD) followed by application of latex modified concrete (LMC) overlay, behave in composite or non-composite fashion and if necessary, specifying the criteria for developing composite action. The motivation behind this study was the fact that some transportation authorities do not allow any structural capacity to be replaced by way of overlay application. Therefore, if a bridge deck is demolished to half depth and then repaired to original depth; it must be structurally rated as if it were only half depth.

As part of the testing, full scale reinforced concrete slabs were subjected to three point bending until failure. Ten of the specimens were cast in the laboratory and four were cut from a decommissioned bridge deck. The depth of overlay varied from approximately half depth of the slab to approximately 1 inch (25.4 mm). Along with depth of applied overlay, one specimen was tested in the inverted position (negative bending) and one specimen had a more conventional AAA concrete mix applied. During each of the tests, measurements were recorded at approximately 1 kip (4.4 kN) intervals. Displacement and strain readings at mid-span were recorded at each of these increments. Strain readings were recovered via DEMEC targets attached at various depths across the cross section and allowed for strain profiles to be generated at each loading interval. The strain profiles along with the cracking patterns were then used to determine if the test specimens exhibited composite or non-composite behavior.

The test results showed that all slabs did behave in composite manner and reached desired strengths, when compared to plane section analyses. Strain profiles remained linear through the interface region indicating that delaminations had not occurred. Cracking patterns also propagated through the interface region without indicating bond damage. Thus, it is recommended that bridge decks repaired by means of HD and application of a LMC overlay be rated as if they are behaving in a composite fashion.

TABLE OF CONTENTS

LIST OF TABLES

LIST OF FIGURES

ACRONYMS

AASHTO	American Association of State Highway and Transportation Officials
ACI	American Concrete Institute
BMS	Bridge Management System
FHWA	Federal Highway Administration
HD	Hydrodemolition
HMWM	High Molecular Weight Methacrylate
LMC	Latex Modified Concrete
LRFD	Load and Resistance Factor Design
MSC	Microsilica Modified Concrete
NDE	Non-Destructive Evaluation
PCC	Portland Cement Concrete
PennDOT	Pennsylvania Department of Transportation
SDC	Super-dense Plasticized Concrete
SHRP	Strategic Highway Research Program
SSD	Saturated Surface Dry

NOMENCLATURE

Δ	Shear interface displacement or slip
ε_s	Shear interface steel reinforcement strain
γ	Normal force factor
μ	Friction factor
ρ	Slab longitudinal steel reinforcement ratio
φ	Curvature
A	Area of material above interface
A_c	Horizontal Area of concrete in the shear span
A_{cv}	area of concrete interface
A_s	Area of tension reinforcement
A_v	Area of steel crossing shear interface
b	Slab width
b_f	Flange width
c	Cohesion factor
c	concrete cover
d_b	Reinforcement bar diameter
d_o	Target depth of Hydrodemolition
f'_c	Concrete compressive strength
f_r	Modulus of Rupture
f_{sp}	Split Cylinder Strength of Concrete

f_y	Steel reinforcement yield strength
h	Height of slab
I	Moment of inertia of gross cross section
K	Generic Limiting factor-Shear Friction
L	Span Length
M	Moment
M_{DL}	Dead load design moment
M_{LL}	Live load design moment
N	Normal Forces
P	Applied Load
Pc	externally applied loads normal to the interface
S	Girder spacing
T	Tension in Reinforcement
t	width of cross-section at the interface
V	Internal shear
V_{ni}	Shear Friction Capacity
w	Shear interface crack width
y	distance from centroid of A to centroid of gross section

U.S. customary units were used throughout this thesis. The following conversion factors were used:

1 inch = 25.4 mm

1 kip = 4.448 kN

1 ksi = 6.895 MPa

Reinforcing bar was also designated using U.S. standard notation. This notation consists of a "#" symbol followed by a number (e.g. #5). The number refers to the bar diameter in eighths of an inch.

1.0 INTRODUCTION AND LITERATURE REVIEW

The objective of this work is to provide laboratory-based experimental verification and assessment of the performance of reinforced concrete deck slabs rehabilitated by means of hydrodemolition (HD) followed by the application of a latex modified concrete (LMC) overlay. The fundamental objective is to determine whether the overlay may be considered composite with the residual deck and if necessary, under what conditions composite behavior may be assumed in eventual load rating of the rehabilitated deck. This work comprises part of a PennDOT funded project.

1.1 CURRENT STANDARDS

Chapter 5 of PennDOT Publication 15[1] *Design Manual Part 4: Structures*, provides guidance for rehabilitation strategies for bridge deck structures (specifically, Figure 5.5.2.3-3). Section 1040 of PennDOT Publication 408[1] *Construction Specifications* provides the necessary specifications and identifies three levels of bridge deck repair (Section 1040.1):

[1] citations are to May 2012 edition of *Publication 15* and April 2011 edition of *Publication 408*

Type 1: Areas where deteriorated concrete extends to a maximum depth of the top of the top mat of reinforcement bars, exposing no more than one-quarter bar diameter.

Type 2: Areas where deteriorated concrete extends beyond the depth of the top of the top mat of reinforcement bars or where reinforcement bars are unbonded. Regardless of the extent of concrete deterioration, A Type 2 repair requires 0.75 in (20mm) clearance be provided all around top mat reinforcing bars (*Pub. 408*. Section 1040.3b)

Type 3: Areas where deteriorated concrete or patching extends to the full depth of the deck, including deck overhang areas.

The focus of the present work is Type 1 and Type 2 repairs carried out by the method of hydrodemolition (HD) followed by the application of a latex modified concrete (LMC) overlay material. The construction requirements for LMC are provided in *Pub. 408* Section 1040.3 and the specifications for LMC and its application are provided in Section 1042. Section 1040.3f.1b provides two methods of executing a Type 2 repair with LMC overlay:

Method 1: provides an LMC overlay (of unspecified, although presumably thin, thickness) on top of a Class AAA concrete repair. This method requires two complete cycles of surface preparation and material application (concrete and LMC), and requires that the AAA concrete achieve a compressive strength of 3300 psi (23 MPa) before subsequent scarification and LMC overlay application.

Method 2: provides that Type 2 repairs up to 2 in. (50 mm) deep may be completed as a single monolithic LMC overlay.

Section 1042.3, to which Method 2 refers, does not, however, appear to specify a maximum thickness of LMC overlay and specifically provides guidance for minimum thickness greater than 2 in. (50 mm) (in Table A, for instance). Clearly Method 2 repairs are preferred. The present study will consider Method 2 Type 2 repairs having LMC overlay depths ranging from 0.5 – 3.25 in. (12 – 83 mm), thereby extending the range of depths of LMC-only repairs from that suggested by *Pub. 408*.

Publication 408 Section 1042.2f requires that latex modified ***mortar*** (LMM) be used for depths less than 1.25 in. (30 mm) and latex modified ***concrete*** (LMC) be used for thicker applications. Mix requirements for both LMM and LMC are provided in Section 1042.2f. Anecdotally, field practice is to use only LMC and place a depth of at least 1.25 in (30 mm).

Both *Publications 408* Sections 1040 and 1042 permit power-driven hand tools, sandblasting or water blasting (i.e.: hydrodemolition (HD)) as a means of surface preparation prior to repair and overlay. Section 1040.3c restricts power tools to those less than 30 lbs (13.6 kg) and limits their use, particularly in cases where reinforcing steel is exposed (i.e. Type II repairs). Hydrodemolition is therefore attractive, particularly where large areas of repair are required.

Both *Publications 408* and *15* are silent on specific requirements for the replacement of reinforcing steel exposed during the HD process. Anecdotally, steel having more than 25% section loss due to corrosion is cut out and replaced. Additionally, PennDOT reports that for LMC applications thicker than about 4 in. (100 mm), an additional layer of welded wire fabric is added, presumably to provide improved crack control.

LMC overlays are reported as having a targeted service life of 20 years (*Pub. 15* Section 5.5.4(a)(3)). Nonetheless, *Pub. 15* Section 5.5.5.1 states that “a latex overlay is not considered

structurally effective" in terms of superstructure load carrying capacity. The primary objective of this study is to challenge this last statement by identifying the extent to which Method 2 LMC overlays used in Type 1 and 2 repairs contribute to the load carrying capacity of the rehabilitated deck slab.

1.2 LITERATURE REVIEW

Approximately 70% of the bridges in the United States have concrete decks (this number is likely higher since 18% of bridge structures have no deck type reported) (FHWA 2011). Concrete overlays provide many benefits for extending the service life of the concrete bridge structure. Overlays can be used to improve wearing surface performance, add load carrying capacity to the structure, and repair regions of concrete damaged by corroding reinforcing steel or other deleterious processes. Overlays are a more time and cost efficient solution than full deck replacement. The objective of this review is to identify best practices and means that may extend the applicability and utility of overlays in lieu of full deck replacement. A recent RILEM (2011) state-of-the-art report, *Bonded Cement-Based Material Overlays for the Repair, the Lining or the Strengthening of Slabs or Pavements* provides an excellent overview of the subject matter.

1.2.1 Overlay Construction Process

The first step in the overlay construction process is to evaluate the concrete deck to determine which portions are in need of repair. Conventionally, an adequate assessment of a deck

will consist of a visual inspection and 'chain dragging' (ASTM D4580-03). The visual inspection will identify cracking, spalling, erosion and other types of physical or chemical deterioration. Other means of non-destructive evaluation (NDE) are available but are rarely used. Harries et al. (2009), provides guidance on appropriate NDE methods for concrete bridge structures.

Once areas of deteriorated concrete are identified, they are removed to a level of sound concrete. There are many different methods for concrete removal on a bridge deck: sandblasting, shotblasting, pneumatic hammers, cutting, explosives, hydro-demolition, etc. (ACI Committee 546 2004). Silfwerbrand (2009) argues that hydrodemolition is the best method of concrete removal. Hydrodemolition (HD) enables concrete to be removed selectively based on the water pressure used. Essentially, water pressure builds inside the concrete and the concrete will begin to spall when the water pressure exceeds the in situ tensile strength of the concrete (Silfwerbrand 2009). Pressure builds in cracks and microcracks in deteriorated concrete and will be resisted in regions of sound concrete removing the former, leaving the latter in place and unaffected. Furthermore, HD can be carried out in a directional manner, making relatively 'focused' concrete removal possible. In addition to being faster and more focused, HD surfaces have a greater exposed aggregate area than other mechanical means of concrete removal enhancing subsequent overlay bond. HD additionally cleans the steel of concrete paste and corrosion product allowing good inspection of steel condition and enhancing bond of the overlay to the newly exposed 'bright' steel. Finally, unlike the use of pneumatic hammers, HD does not result in vibrations which may result in microcracking of the exposed surface.

Once damaged concrete is removed, the exposed concrete must be cleaned and prepared to accept the overlay. The purpose of cleaning and prepping the concrete substrate concrete is to

ensure that there will be a sound monolithic connection between the substrate and the concrete overlay. Cleaning removes dirt and laitance that will affect the performance of the overlay. Common concrete surface cleaning techniques include sandblasting, shotblasting and high-pressure water blasting (Vaysburd and Bissonnette 2011). These methods not only clean the concrete of debris but also leave behind a rough and relatively uniform surface on the substrate concrete. The roughness of the substrate level provides the mechanical bond crucial for good overlay performance. The amplitude of the resulting substrate should be relatively uniform across the surface (to avoid stress raisers) and be sufficient to fully engage the coarse aggregate in the substrate concrete.

Similarly, exposed reinforcement steel must be cleaned, inspected and possibly replaced prior to placement of the overlay. Cleaning of reinforcement usually occurs during the concrete surface cleaning procedures but practitioners should pay careful attention to the reinforcement condition once it is exposed (Vaysburd and Bissonnette 2011). Standard practice dictates that epoxy coated reinforcing steel should be recoated prior to overlay placement. Where reinforcing steel is found to be corroded, the source or cause of corrosion should be determined. In some cases removing and overlaying [usually chloride] contaminated concrete will simply initiate corrosion immediately adjacent the patched region (Vaysburd and Bissonnette 2011). Thus remedial measures such as cathodic protection are necessary in addition to the overlay if long term performance is to be assured.

Another advantage of the use of overlays is that there is minimal need for formwork or falsework since the substrate deck remains intact. For relatively thick overlays that project above the original slab thickness (i.e.: cover to existing top steel is increased over that in the original

deck), additional reinforcing steel (usually a welded wire fabric mat) should be provided to provide shrinkage and temperature crack control. Research has shown that reinforcing steel in concrete overlays performs just as well in pull-out tests as reinforcement placed at mid-thickness of a conventional concrete slab (Fowler and Trevino 2011).

Concrete overlays are generally selected to have similar mechanical properties as the sound substrate concrete (Silfwerbrand 2009). Latex modified concrete (LMC) is the preferred overlay material due to its low permeability and better bond to the substrate concrete (Fowler and Trevino 2011). Selection of an LMC overlay comes with inherent benefits of having mixing and batching controls that are generally more controlled than for conventional concrete. More stringent quality control should ultimately lead to having a better performing overlay.

Like any concrete flatwork, there are a variety of environmental factors during placement and cure that must be controlled. High initial evaporation rates lead to plastic shrinkage cracks. Additionally, since the overlay is supported by, and eventually is expected to be composite with the substrate concrete, large temperature gradients or differentials that may result in thermal cracking of large overlay areas and should be avoided. For this reason, overlay placement is often conducted overnight rather than in daylight. Conventional best curing practices, such as curing blankets and membranes, are appropriate for overlay construction.

If proper construction techniques are followed, concrete overlays can be a very effective way to repair bridge decks. All stages of overlay construction can impact the ultimate performance of the overlay. However current best practices, as described briefly in section 1.2.4 will result in sound overlay performance.

1.2.2 Interface Stresses

Sound bond between the substrate and LMC concrete is crucial to maintaining composite action. The stresses that occur at the interface are complex due to the irregularity of the interface and complexity of loading (Silfwerbrand 2009). Fundamental mechanics of a slab in flexure, however, allow the interface stresses to be assessed. Horizontal shear must be engaged to transfer the principal horizontal tension and compression forces: this is a so-called VAy/It shear. The tension force developed in the reinforcing steel shear is resisted over the interface area of the shear span. Due to the self-weight of the overlay and the fact that transient loads are applied to the top of the overlay, the interface region is also subject to compression, which enhances the shear transfer. Loading that would result in tension across the interface is unlikely.

Shear transfer across a concrete interface is termed ‘shear friction’. Shear friction theory is based on an interface having perpendicular reinforcement to provide ‘clamping’ of the interface. While no perpendicular reinforcement is present in an overlay application, the overlay self-weight and transient gravity loads also serve to provide clamping of the interface to some degree. Thus looking to shear friction approaches for guidance in assessing overlay interface capacity is appropriate.

There are three mechanisms of shear friction resistance: cohesion, aggregate interlock, and clamping force. Figure 1 provides a schematic representation of shear friction as originally proposed by Birkeland and Birkeland (1966).

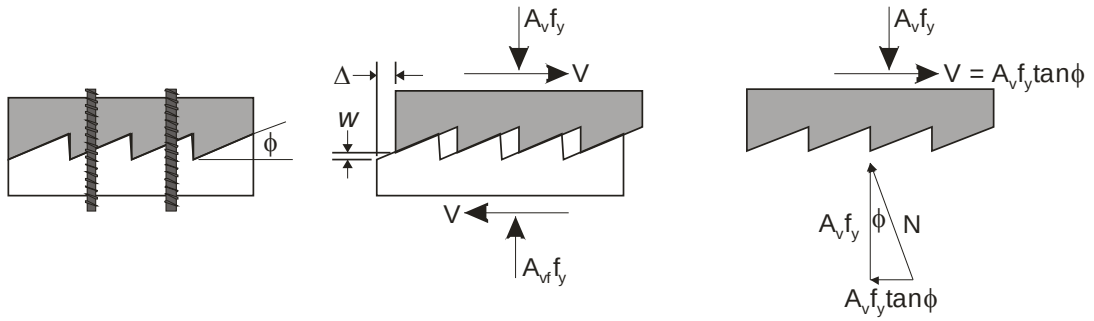

1.0a)Cohesion 1b) Aggregate Interlock 1c) Clamping Force

Figure 1: Saw-toothed model for shear friction. (redrawn based on Birkeland and Birkeland 1966)

Cohesion is the pre-cracked shear resistance of the concrete. Aggregate interlock is engaged after the cohesive capacity is exhausted and the interface cracks. In order for a shear crack to displace (Δ), the rough surfaces must pass over each other resulting in a corresponding crack opening (w). This is resisted by 'interlock' of the rough surfaces and enhanced by normal forces (N) (thus, the use of the term 'friction'). The clamping force is provided by reinforcing steel crossing the interface. As the interface crack displaces, the steel is placed in tension, resulting in a clamping force proportional to the resulting steel stress. Provisions for establishing shear friction capacity assume that cohesive bond is negligible (i.e.: the concrete interface is cracked) and that the maximum aggregate interlock and steel clamping forces act simultaneously. This last assumption is not true. The aggregate interlock is initially high and degrades as the interface slips. The slip, however is what engages the steel clamping force. Thus, as shown by Zeno (2009), the aggregate interlock reaches a maximum value and degrades while the clamping force is relatively low and increases. The clamping force is ultimately limited by the yield capacity of the reinforcing steel, however without very large interface slip (exceeding about 0.1 in.), this theoretical maximum clamping force is not achieved (Zeno 2009).

Most shear friction recommendations take the form of Equation 1:

$$V_{ni} = cA_{cv} + \mu A_v f_y + \gamma P_c \leq KA_{cv} \quad (1)$$

where: V_{ni} = shear friction capacity

A_{cv} = area of concrete interface

A_v = area of reinforcing steel having yield strength equal to f_y crossing interface

P_c = externally applied loads normal to the interface

Table 1 presents shear friction parameters, c, μ, γ and K, from AASHTO (2010), ACI 318 (2011) and two related scholarly works. The equation terms and limits associated with the concrete interface area, A_{cv}, in each case, are the *implied* contributions of aggregate interlock to the shear friction capacity. These provide guidance as to the anticipated shear capacity at the substrate-overlay interface. While the concept of shear friction requires a normal force, this is provided in the case of an overlay by its self-weight and the transient loads resulting in the interface shear. All cases presented in Table 1 assume "normal-weight concrete placed against a clean concrete surface, free of laitance, with surface intentionally roughened to an amplitude of 0.25 in.(6.35 mm)" (AASHTO 2010).

Table 1: Shear Friction Coefficients and Implied Aggregate Interlock Shear Capacity

Source	c	μ	γ	K	implied aggregate interlock interface capacity
AASHTO (§5.8.4)	240 psi (1.65 MPa)	1.0	1.0	$0.25f_c' \leq 1500$ psi (10.3 MPa)	240 psi (1.65 MPa)
ACI 318 (§11.6.4)	0	1.0	0	$0.20f_c' \leq 800$ psi (5.52 MPa)	-
Kahn and Mitchell (2002)	$0.05f_c'$	1.4	0	$0.20f_c'$	$0.05f_c'$
Harries, Zeno and Shahrooz (2012)	$0.06f_c'$	$0.0014E_s$	0	$0.20f_c'$	$0.06f_c'$
f_c' = concrete compressive strength E_s = modulus of elasticity of reinforcing steel					

The implied aggregate interlock capacities shown in Table 1 are very similar. The recommendations of Kahn and Mitchell (2002) were developed for high strength concrete having values of f_c' up to 14000 psi (96.5 MPa) while those of Harries et al. (2012) were based on experiments in which f_c' varied from 5000 to 7000 psi (34.5 – 48.3 MPa).

1.2.3 Defining Bond and Methods of Testing Bond Strength

Bonded Portland cement overlays, like unbonded overlays, provide water and corrosive agent protection to underlying structurally sound concrete. Bonded overlays, however are not intended to be 'sacrificial' rather they should act in a composite manner with the substrate concrete, restoring, or even improving, the original monolithic slab capacity.

As described previously, bond between the overlay and substrate has two components: chemical adhesion and mechanical interlock (Silfwerbrand et al. 2011). Chemical adhesion results from a well-prepared substrate interface while mechanical interlock results from the physical

irregularities at the interface. Adding bonding agents to Portland cement can improve adhesion. Portland cement grout with latex or certain epoxy resins can be added to the overlay concrete mixture to improve adhesion. Using such additives, however, comes with inherent risks, including creating a thin interface between the substrate and overlay introducing two potential planes of bonding (Silfwerbrand et al. 2011). Additionally, latex additives have been associated with finishing problems that have led to shrinkage cracking (ACI Committee 546 2004).

Mechanical interlock stems from the roughness of the interface. The sand area method is a simple manner of quantifying this roughness. This method involves pouring a known volume of sand over the concrete surface. The sand is spread over the concrete in a circular fashion until all the cavities on the concrete surface are filled. A smaller circle correlates to a rougher concrete surface (Silfwerbrand 2009).

Bond strength is usually assessed by means of a tensile pull off tests (ICRI 2004; ASTM C1583-13). A pull off test involves isolating a region of the substrate-interface-overlay region using a hole saw (core drill). A test fixture (dolly) is affixed to the overlay and a monotonic concentric tension force is applied until tensile failure of the isolated specimen results. Figure 2 provides a schematic representation of the pull off test and the failures that may result. There are a variety of available fixtures reported to be suitable for such testing. Vaysburd and McDonald (1999) provide a review of available fixtures and specimen sizes. Eveslage et al. (2010) and others adopt the rule-of-thumb that the specimen size must exceed the maximum coarse aggregate size.

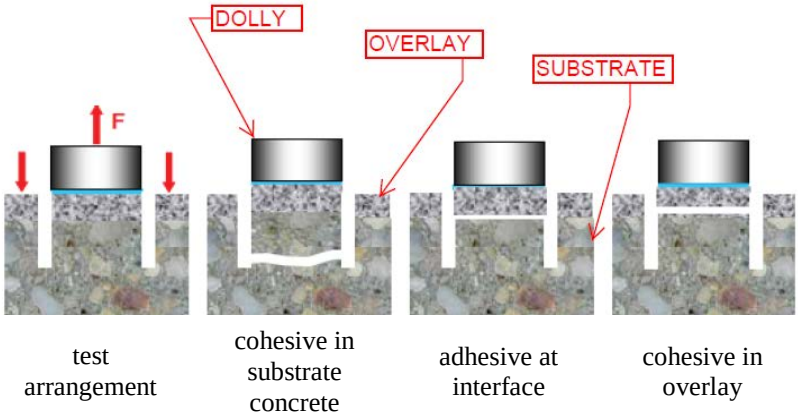

Figure 2: Bond Strength Pull-off Test (adopted from Germann Instruments Inc.)

Failure in a pull off test will occur through the weakest material. A cohesive failure in the substrate concrete is the preferred failure mode since this indicates that both the overlay and the interface bond exceed the substrate concrete tensile strength. As a repair, the substrate material properties essentially limit the outcome of such a test since these are the only values that one has no control over in the design of the repair.

Direct tension is not representative of in situ forces on an overlay system however the pull off test is a simple and viable test for quality assurance. Studies have indicated that the tensile bond strength found through the pull off method is less than the shear strength of the interface. Gillum et al. (2001) reports tensile strength approximately 35% of shear strength while Silfwerbrand (2009) report the value to be approximately one half of the shear bond strength. There is conflicting available guidance on the minimum substrate tension capacity from pull-off tests: Wenzlick (2002) suggests a minimum of 100 psi (0.69 MPa), Basham (2004) recommends 200 psi (1.38 MPa), while ICRI (2004) suggests a value below 175 psi indicates poor bond.

1.2.4 Factors Affecting Bond

A monolithic connection in a bonded concrete overlay is achieved through several avenues some of which have greater importance than others. Silfwerbrand (2009) lists the five most important factors affecting the performance of this interface as: absence of microcracks, absence of laitance, cleanliness, compaction of overlay, and curing. The following is a summary of Silfwerbrand's list of factors in chronological order as they occur in the overlay process. Relative importance is given by Silfwerbrand on a scale of 1 through 3 in which 3 is most important.

Substrate Properties (1) Mechanical properties of the substrate concrete include the modulus of elasticity, tensile strength and compressive strength. Silfwerbrand (2009) states that composite action of the overlay is best achieved when the overlay properties are designed to closely match those of the substrate concrete.

Microcracks (3) Microcracking is often caused by the method by which deteriorated concrete is removed. Pneumatic hammers are likely to cause more microcracking than other non-impact alternatives, such as hydrodemolition. Regions of microcracks are potential weak zones in which adequate bond strength will not develop.

Laitance (3) Laitance is a layer of fine particles that forms as excess water bleeds to the surface of the concrete during the curing process. Laitance is only an issue when bonding to an existing concrete surface; when any form of demolition is used to remove the substrate concrete, laitance is removed.

Roughness (1) As discussed above, bond strength is developed partially by mechanical interlock. To a degree, the 'rougher' the substrate level is, the more mechanical interlock is able to develop. This factor is highly dependent on the method of removing deteriorated concrete.

Cleanliness (3) This factor is perhaps one of the most important and most easily controlled. Both ACI Committee 546 (2004) and Silfwerbrand (2009) agree that surface cleanliness is critical to performance of the repair. Supporting evidence has been found in Sweden, where bonded overlays were used on two bridge decks. The overlays did not perform well due to loose particles found at the interface between the substrate and overlay. These loose particles resulted in poor bond strength (Silfwerbrand et al. 2011).

Prewetting (2) Bond strength is maximized when the substrate surface to which the overlay is applied is saturated and then allowed to superficially dry prior to overlay placement. Silfwerbrand (2009) recommends keeping the substrate wet for 48 hours then letting it dry for 12 hours preceding the overlay placement. This condition is known as saturated, surface-dry (SSD) and is intended to minimize the amount of water that the substrate will wick away from the overlay when it is placed. Conventional practice is similar although the substrate is maintained wet, without standing water; a condition referred to as saturated, surface-wet (SSW). Vaysburd et al. (2011) recommends that the SSD condition be used when testing for the optimum water condition of the substrate cannot be done.

Bonding Agents (1) Silfwerbrand (2009) argues against using bonding agents such as epoxy and grout because they create multiple interfaces, thus increasing the probability of a weak bond.

Overlay Properties (2) Overlay mix design can affect bond strength in the same way as substrate properties. Workability, strength and other products of the mix design can have effects on overall overlay performance.

Placement (1) As with all concrete construction, poor placement techniques can lead to segregation within the overlay.

Compacting (3) Proper compaction leads to fewer and better distributed air voids at the interface. Air voids can detrimentally affect bond strength and result in poor overlay performance.

Curing (3) As in any concrete flatwork construction, improper curing can lead to surface cracks which, while having little effect on bond to the substrate, nonetheless result in poor-performing overlay.

Time(2) and Early Traffic(1) Time and early traffic loading are factors that work hand in hand. If traffic is applied too early, vibrations may cause differential movements between the overlay and the substrate. Studies have shown that bond strength develops at a rate similar to compressive strength (Silfwerbrand 2009). If enough time is allowed for bond strength to develop, composite action should be developed.

Fatigue (1) Low-cycle fatigue tests conducted at high stress levels have shown that bond is not a weakness in the overlay system. Silfwerbrand (2009) comments that provided the static bond strength is adequate and the tension reinforcement does not coincide with the bond interface, fatigue performance is not an issue. There is no known data for high cycle fatigue which is the *in situ* condition of an overlay.

Environment (1) Environmental factors, such as temperature, should be taken into consideration during any concrete placement operation including overlay placement.

1.2.5 Experimental Studies of Bond Strength

Several studies have focused on overlay-to-substrate bond strength. The following general conclusions have been drawn:

- Bond strength plays a very important role in overall performance when the interface area is subjected to longitudinal compression (from positive bending of the slab). When the interface is subjected to tension (negative bending areas), bond strength does not play as vital a role in overlay performance.
- Construction procedures, such as the method of concrete removal, affect overlay performance.
- Sealants used on the substrate surface reduce bond strength.

Gillum et al. (1998) present a Comprehensive study performed for the Ohio Department of Transportation investigated bond performance of overlays over concrete sealed with high molecular weight methacrylate (HMWM) and epoxy. The report indicates a limited number of previous studies addressing the effects of substrate surface preparation on bond strength. Critically, the authors report that there are no known studies to determine the bond strength needed for an overlay to be deemed effective. Both field and laboratory specimens were used in a variety of tests: direct shear, direct tension (pull-off), Strategic Highway Research Program (SHRP) interfacial bond and flexural beam tests. Of particular interest are the flexural beam tests, which consisted of a one half-scale model of a 12 in. (300 mm) strip of typical bridge slab. Overlays used on these specimens were 1.6 in. (40 mm) deep microsilica modified concrete (MSC) overlays. These flexural specimens were subjected to both negative and positive bending. Overlays in positive bending failed as a result of bond failure of the overlay whether the specimens were sealed or not. Figure 3 shows to examples of failures associated with poor overlay bond (from Cole et al. 2002). Negative bending did not cause specimens to fail due to bond failure since the overlay is in tension (Figure 4).

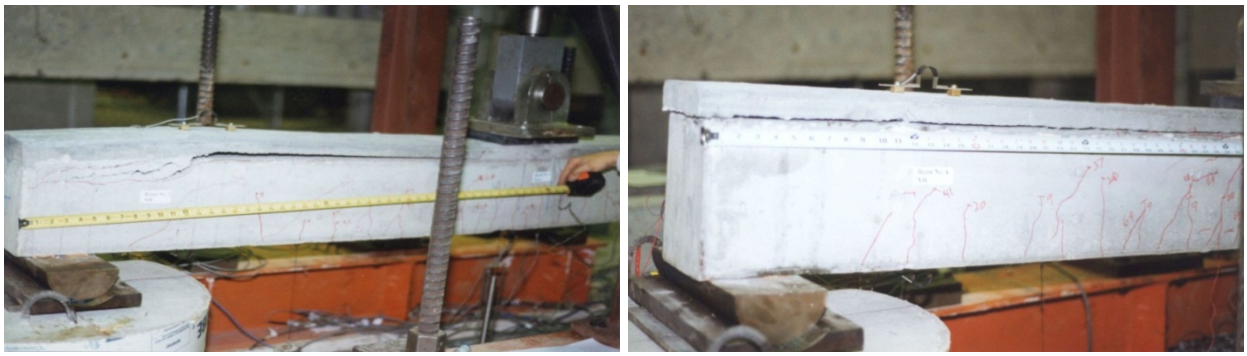

a) 'buckling' failure of overlay in compression

b) 'slip' failure of overlay characterized by relative movement at the ends of the test slab

Figure 3: Examples of Bond Failure of Overlays Subject to Positive Bending (Cole et al. 2002).

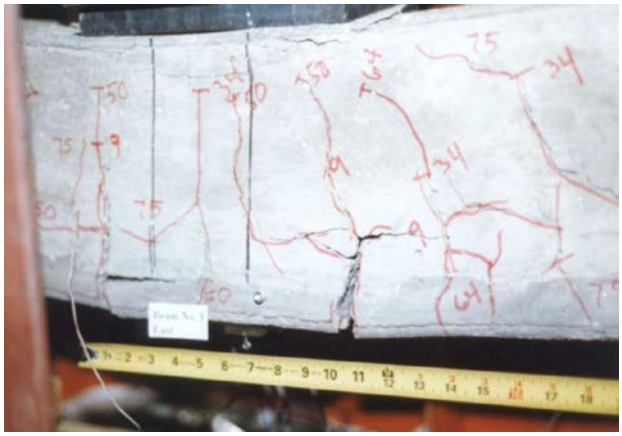

Figure 4: Example of Overlayed Slab in Negative Bending - Overlay at Bottom of Test Slab in Tension Zone (Cole et al. 2002)

Gillum et al. (2001) continued, focusing on whether the application of low-viscosity sealers affected the bond between Portland cement-based overlays and bridge decks. Bond strength was again tested under four different types of tests: direct shear, direct tension, SHRP interfacial bond and flexural beam tests. Microsilica modified concrete (MSC), super-dense plasticized concrete (SDC) and latex modified concrete (LMC) were tested in both field and laboratory conditions. For the field tests, it was determined that results from the direct tension test are approximately 35%

the values of direct shear tests. Additionally, there was a high level of scatter in bond strength values for the LMC overlay making determination of the bond strength, in this case, uncertain. Laboratory tests included test beams intended to replicate an overlay bonded to a bridge deck. Flexural tests in both positive and negative three point bending revealed that the overlay seemed to be adequately bonded to the substrate concrete for the case in which no sealer had been applied to the substrate. LMC was found to have the highest bond strength among the three alternatives: 860 psi (5.93 MPa). Four primary conclusions resulted from the study: 1) flexural testing is the most realistic method of testing specimens; 2) sealers reduce bond strength by approximately 50% when compared to unsealed specimens; 3) sandblasting the interface where sealers are applied can increase bond strength of sealed specimens to 80-85% of unsealed specimens [although it must be suspected that the subsequent sandblasting simply removes the applied sealer]; and 4) in negative moment regions it is not as crucial to sandblast sealed areas as it is in positive bending regions, i.e. bond strength is not as significant a concern in negative moment regions such as over piers.

Cole et al. (2002), in a continuation of the Gillum et al. (2001) study, considered overlays placed over sealed concrete bridge decks; their performance was evaluated in both static and fatigue loading scenarios. Specimens consisted of one-third-scale subassemblages of a steel stringer bridge. HMWM sealers and gravity-fed epoxy resins were found to reduce bond strength by approximately 50%. Sandblasting once the sealer had cured can restore bond strength to 80 to 85% of that without sealers (once again, one suspects that the sandblasting is simply removing the sealer). Broadcasting sand at a rate of 1 kg/m^2 immediately after sealer application was also shown to restore bond strength. Bond strength is a function of bending direction. Specimens subject to positive moments exhibited bond failure when sealers were used; bond failure was mitigated when sealers were not used. Specimens subject to negative moments, once again, did not exhibit these

failures due to the fact that the interface area is located in the region of flexure-induced tensile stresses. Fatigue testing to 1,000,000 cycles showed that sealers were not detrimental to the overlay performance provided sand is applied to the sealer as it cured.

Wenzlick (2002) reports a study by the Missouri Department of Transportation conducted in an effort to support the use of hydrodemolition as the preferred method of concrete removal prior to subsequent concrete overlay. Both latex modified and silica fume overlays were considered. The study focused on time, cost and performance of hydrodemolition and compared it to conventional pneumatic hammer removal of concrete. Specimens came from decommissioned bridges and bond strengths were determined using direct tension tests. Hydrodemolition was able to reduce micro-fractures at the substrate level concrete, which ultimately was deemed to result in better overlay bond strength. Bond strength of the overlay installed following hydrodemolition ranged from 121 to 161 psi (0.84 – 1.11 MPa), averaging 151 psi (1.04 MPa), whereas pneumatic hammering and milling averaged 80 and 140 psi (0.55 and 0.97 MPa), respectively.

Alhassan and Issa (2010) demonstrated the superiority of synthetic fiber latex-modified concrete overlays over other overlay types. Full scale testing was conducted on a two-span prototype bridge having two equal 40 foot (12.2 m) spans. Various AASHTO loading scenarios were tested and it was found that the load-deflection response was improved as a result of overlay application: increasing the 8 in. (200 mm) deck depth with a 2.25 in. (55 mm) thick fibrous LMC overlay was found to increase the stiffness of the composite bridge by 20%. This improved behavior was attributed to composite action between the substrate concrete and the overlay. Composite action can only be developed through adequate bond strength. The complexities of

analyzing stresses at the overlay-substrate interface were also discussed, with several finite-element analyses performed to validate critical issues found in experimental test results.

Silfwerbrand (2009) and Silfwerbrand et al (2011) report extensive ongoing research and implementation of concrete overlays for the repair of bridge decks in Sweden. During the late 1980s and early 1990s, bond strength tests were performed on 20 bridge decks that had been hydrodemolished and repaired with a bonded concrete overlay. The majority of these tests did not fail at the interface and failure strengths averaged over 217 psi (1.5 MPa). Silfwerbrand argues that since most of the specimens did not fail at the interface between overlay and substrate level concrete, the actual bond strength is higher than the recorded values. Most specimens failed within the substrate level concrete. Bridges with newer overlays performed slightly better than older overlays in terms of both failure strengths and percentage of bond failures. Silfwerbrand attributes this to contractors, who work in the bridge deck repair arena, recognizing that careful attention must be paid to construction procedures, such as surface preparation.

1.3 SUMMARY

LMC overlays, when correctly constructed, can increase deck capacity, improve deck surface conditions, and provide a long-term lower maintenance solution for repairing degraded concrete deck structures. Appropriate repair and maintenance procedures are those that reduce manpower requirements, time, resource use, and shut-down times. In addition to addressing these issues, LMC deck overlays are also favorable with respect to sustainability when compared to other methods of repair or full deck replacement (Silfwerbrand 2009). Overlay performance is

governed mostly by bond of the overlay to the substrate concrete. Good bond is primarily affected by good construction practices in preparing the substrate and installing the overlay. A well-designed and constructed overlay should restore a moderately degraded deck – represented by a Type 1 or Type 2 repair – to its original structural capacity and have a service life on the order of 20 years or more (*Pub. 15* Section 5.5.4(a)(3)).

2.0 REVIEW OF INSPECTION DATA

2.1 GENERAL PERFORMANCE OF LOCAL OVERLAYS

A review of available inspection reports and construction documents was carried out to assess the condition and performance of latex modified concrete (LMC) overlays in the local PennDOT district (District 11). The review was carried out in February 2013. Initially, the bridge management system (BMS) was queried to identify bridges within the district that had a LMC overlay applied. This search returned 149 bridges (8% of those in D11) representing over 3 million square feet (280,000 m^2) of deck area (20%). Overlays (based on 'year of reconstruction') range from less than one year to 40 years old. Wearing surface thicknesses of up to 3.5 in. (8.9 mm) were reported. Wearing surface ratings range from 4 to 9 with the majority of ratings at or above 6 as shown in Figure 5. Figure 6 plots the wearing surface ratings against the reported year of reconstruction. As one would expect, bridges repaired more recently had slightly better wearing surface ratings than those with older repairs (as shown by trendline in Figure 6).

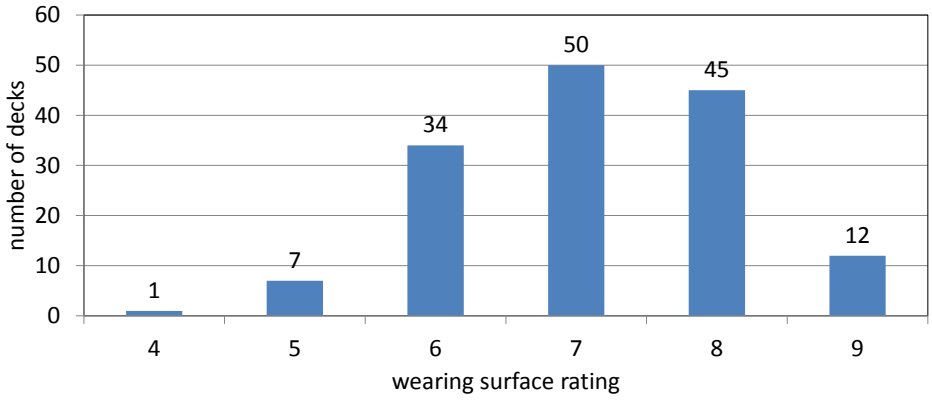

Figure 5: Distribution of wearing surface ratings for LMC-Overlayed Bridge Decks

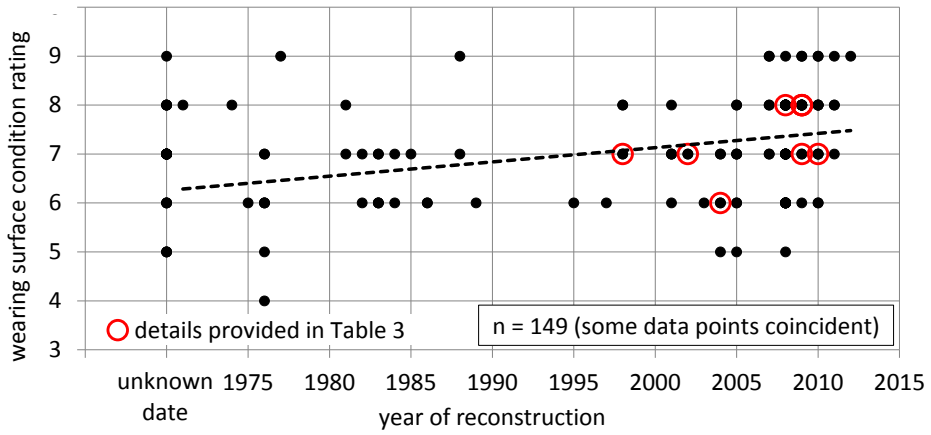

Figure 6: Wearing Surface Condition vs. Year of Reconstruction for LMC-Overlayed Bridge Decks

A qualitative review of all comments associated with deck and overlay performance of the 149 sample decks was undertaken; the results are shown in Table 2. Keywords were used to classify the condition of the overlay ("good", "fair" and, "poor"); the extent of cracking ("minor" or "few", "moderate", "widespread" or "numerous", and "severe"); and evidence of surface wear (reported or not). Considering the nature of inspection comments, it is believed reasonable to assume that there were no observed issues if there was no mention of an issue. That is, while 64 of 149 overlays were considered to be "good"; there was no mention of condition in 77 reports – one may assume, therefore, that close to 141 of the 149 decks were "good" or had no condition issues meriting comment.

Considering the 40 cases indicated as having moderate or severe cracking (Table 2), the following observations are made:

- Most comments (30 of 40) refer to ‘hairline’ or ‘map’ cracking; both are possible indications of shrinkage cracks associated with inadequate cure conditions (see, for example, Figures 7a, b and d).
- Many comments (18 of 40) refer to longitudinal cracking (see, for example, Figure 7f); this may be reflective cracking at girder locations although this cannot be confirmed.
- Some comments (10 of 40) refer to transverse tracks. Without further data it is not possible to assess a likely cause of these, but shrinkage restraint cannot be ruled out.

Overall, the 149 decks with overlays in District 11 are performing well. No major issues for concern are noted. Much of the observed cracking is very likely associated with early-age effects resulting from inadequate curing processes.

Table 2: Qualitative Review of Inspection Comments[1] Related to Overlay (n=149)

overall condition of overlay	*good*	*fair*		*poor*	no mention
	64	7		1	77
extent of cracking of overlay	*minor* or *few*	*moderate*		*severe*	no mention
	60	36		4	49
reported nature of cracking		*hairline* or *map cracking*	*longitudinal cracking*	*transverse cracking*	
		30	18	10	
evidence of surface wearing	reported				no mention
	28				121

Note: terms in *italic* text are search words used to categorize qualitative inspection data

Inspector comments associated with the poorly performing decks identified in Table 2 include:

Single deck having ‘poor’ condition of overlay: “New modified latex overlay installed since 2010 inspection. A 100'L [length] of the SB [southbound] passing lane exhibits poor quality concrete, close-density pop-outs were observed within a 100' length of deck in span 4. Additionally, several

3' length longitudinal hairline cracks were found propagating through a section of haunch adjacent to the center joint, no other problems were noted." (reported year of overlay: 2011; deck rating in 2012: 7) This comment appears to indicate a substandard LMC installation.

Four decks having 'severe' cracking: **"**Condition rating of the latex modified concrete surface was reduced to Satisfactory, minor deterioration was noted. The left lane has moderate-to-heavy density hairline map cracks." (reported year of overlay: 1982 (more likely 2008 based on incomplete BMS data); deck rating in 2012: 6)

"Integral concrete - heavy longitudinal, map, and transverse cracking." (reported year of overlay: 1995; deck rating in 2012: 6)

"New latex overlay - heavy wide spread hairline map cracking in passing lane and on both shoulders, minor hairline map cracking in travel lane. No plans exist for this wearing surface at time of inspection, actual thickness is unknown." (reported year of overlay: 2008; deck rating in 2012: 7)

"Latex concrete overlay - minor to moderate wear in wheel paths, severe transverse and longitudinal cracking." (reported year of overlay: 1989; deck rating in 2012: 6)

None of these comments highlight any significant issues; simply general deterioration of overlays.

2.2 BRIDGES FOR DETAILED STUDY

In consultation with District 11, nine bridges were selected for further examination; these are reported in Table 3 with the specific bridge identification removed. Inspection reports and available construction documents were reviewed to establish the data shown. Values of overlay

depth vary considerably and are not necessarily consistent with that reported in the BMS (Bridge Management System). The depth values given in construction documents are assumed to be target depths and likely the basis for calculating pay-quantities. Where available, depth-check records maintained by inspectors were reviewed. In most cases spot-depths varied both along and across bridge decks. In some cases, spot depths exceeded two or three times the reported depth. This is likely the result of the requirement to provide hydrodemolition to a ‘depth of sound concrete’. Photographs of many of the decks considered, taken January 2013, were provided by PennDOT District 11. Representative photos illustrating the notes on each deck are provided in Figure 7. Additional photos from two of these bridges are provided in Figure 8. These show a damaged LMC overlay at the acute angle of a skew (Figure 8a), an apparent pop-out (Figure 8b), and a mortar patch of an LMC overlay (Figure 8c).

Apart from some localized damage on Bridge F, no significant areas of concern were identified in the bridges selected for detailed study.

Table 3: Summary of Inspection Data

ID	A	B	C	D	E	F	G	H	I
Year of LMC overlay	2002[1]	2008	1998	2009	2009	2004	2009	2009	2010
Type of LMC	-	-	type 1 PCC	conventional LMC	conventional LMC	conventional LMC	rapid set	rapid set	conventional LMC (span) rapid set (S. approach)
Reported depth of HD	-	0.25 in.	0.25 in.	varies: to sound concrete	varies: to sound concrete	varies: to sound concrete	1.50 in.	1.50 in.	1.00 in.
Depth of LMC (construction records)	1.25 in.	1.25 in.	1.5 in.	varies: LMC to increase slab depth 0.5 in.	varies: LMC to increase slab depth 0.5 in.	varies: LMC to match extant elevations	1.5 in., 3.5 in. and 4.5 in.	1.5 in., 3.5 in. and 4.5 in.	1.50 in.
Depth of LMC (BMS)	1.2 in.	0.5 in.	1.20 in.	1.0 in.	0.5 in.	1.5 in.	3.0 in.	3.0 in.	0.5 in.
MPT at LMC placement	-	-	half width closures	one lane maintained	one lane maintained	traffic during project	single lane closures	single lane closures	traffic during project
7 day LMC strength	-	-	4260 psi	-	-	4050-6800 psi	-	-	5 day: 3000 psi
28 day LMC strength	-	-	3200-5900 psi	4140-7240 psi	4140-7241 psi	-	3000-4000 psi	3000-4000 psi	3500 psi
Wearing Surface Rating	7	8	7	8	7	6	8	8	7
Deck Rating	7	9	-	7	7	4	-	-	-
Notes	A	B	C	D	E	F	G	H	I
Figure	7a	7b	7c	7d	7e	7f	-	-	-

Notes for Table 3

The following notes are transcribed directly from District 11 inspection reports:

A. several minor cracks (see Figure 7a)
B. minor hairline cracks (see Figure 7b)
C. Integral concrete - moderate wearing and light cracking typical of all spans. Small popouts have been patched with mortar (Figure 8c shows image of deck; no popouts are seen)
D. few small areas of hairline cracking (see Figure 7d)
E. LMC overlay-good condition (see Figure 7e)
F. LMC - fair condition - numerous hairline longitudinal cracks (see Figure 7f)
G. The latex-modified concrete wearing surface exhibits a few longitudinal hairline cracks and small diameter shallow concrete spall.
H. The 3 in. (76.2 mm) thick latex-modified concrete wearing surface was recently replaced as part of the Ft. Duquesne Bridge and Ramp Rehabilitation project and is in very good condition.
I. The Latex Modified Concrete (LMC) wearing surface is in overall good condition. Areas of moderate density hairline mapcracking are present in the northbound right lane and shoulder areas throughout. Multiple longitudinal hairline cracks are present throughout the northbound right lane for the full length of the bridge. Random transverse hairline cracking is present throughout. Span 10 Northbound deck right lane exhibits a 6 inch (152.4 mm) diameter by 3/4 inch (19.1 mm) deep shallow spall. The deck wearing surface at Pier 12 is chipped along the sawcut paving joint with missing joint filler. No significant change in the wearing surface has been noted since the 2011 Deck Wearing Surface cracking inspection.

a) Minor hairline cracks (Bridge A)

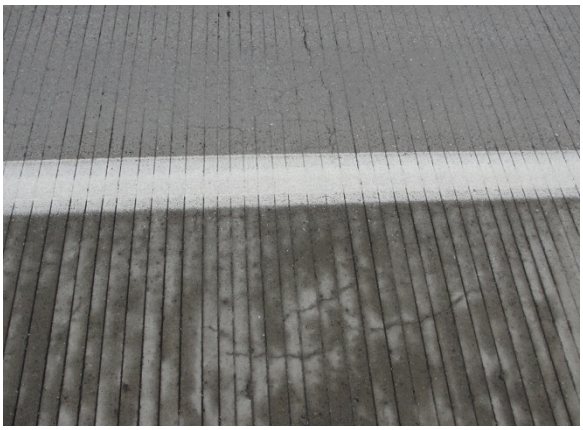

b) Minor hairline cracks (Bridge B)

c) LMC Overlayed Deck of Bridge C
(photo taken 1.14.13)

d) Minor Hairline Cracks (Bridge D)

e) LMC Overlayed Deck of Bridge E

f) Hairline Longitudinal Cracks (Bridge F)

Figure 7: Photos Reflecting Inspection Notes For Bridges Reported in Table 3

a) Damage to LMC overlay at location of acute skew (Bridge D)

b) Apparent Pop-out of LMC (Bridge F)

c) Mortar Patch of LMC (Bridge F)

Figure 8: Observed Local Damage to LMC Overlays

3.0 EXPERIMENTAL PROGRAM

The experimental program consisted of two different sets of slabs: laboratory-cast specimens, and specimens recovered from a decommissioned bridge (Marshall Ave. slabs). Geometry and material properties differed between the two sets of specimens, but the HD and subsequent LMC installation procedures were the same. The testing procedures were also the same with the exception of span length and loading increments. Details of the testing program are provided in the following sections.

3.1 SPECIMEN DETAILS AND TESTING MATRIX

3.1.1 Laboratory Specimens

Ten 90 in. (2286 mm) by 22 in. (559 mm) slabs, each 7.5 in. (191 mm) deep were cast. Figure 9 provides details of the control specimen (Slab A; not receiving LMC). The primary flexural reinforcing (i.e.: bridge transverse) steel shown in Figure 9b was bent as a closed tie in order to ensure full development of both top and bottom steel. Straight secondary reinforcing (bridge longitudinal) steel was placed within the primary steel ties. Figure 10 shows the slab reinforcing cages positioned within formwork, prior to concrete placement.

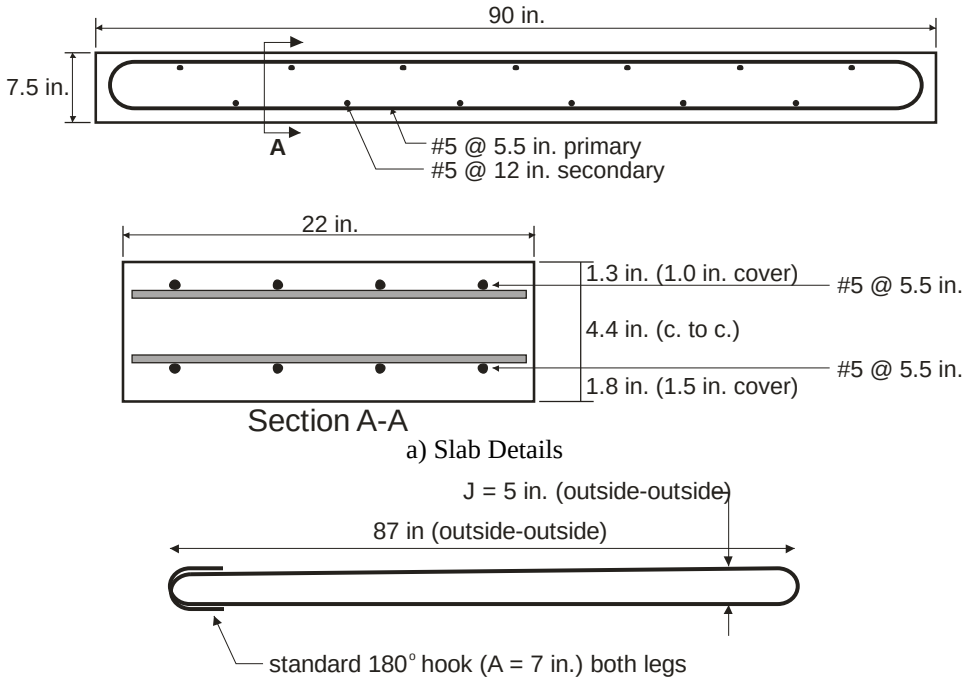

a) Slab Details

b) #5 Primary Reinforcing Steel Bend Detail (Installed in Alternating Directions)

Figure 9: Details of Laboratory Specimens (Slab A as Tested)

Figure 10: Laboratory Slab Forms Prior to Placing Concrete

The testing matrix for the laboratory specimens begins with Slab A as the control (see Figure 9). The remaining slabs were subject to removal of their top surface by hydrodemolition (HD) and overlaying the affected region with latex-modified concrete (LMC) as shown

schematically in Figure 11. The primary variable in this study is the depth of the HD and subsequent LMC overlay, d_o. Figure 12 provides the as-built slab details for Slabs B through H, all receiving LMC overlays. The 'target' depths of HD and LMC (d_o) were based on the concrete cover, c, and bar dimensions, d_b, and are noted in Figure 12. For example, the target depth of HD for Slab D is $d_o \approx c + d_b$; thus the depth of HD should be at the intersection of the primary and secondary reinforcing steel in this section.

Figure 12 indicates the average measured depth of LMC calculated from the recorded depths from six measurement points across the approximately 66 x 22 in. (1676 x 559 mm) extent of HD (Figure 11) as recorded in Table 4. These depths were measured perpendicular to a level placed across the top of the formwork prior to LMC placement. This method is similar to that used by PennDOT to record such depths in the field. In order to be consistent with field practice, a minimum depth of LMC was provided; this required increasing the overall depth of Slabs B and C to 8.5 and 8 in. (216 and 203 mm), respectively.

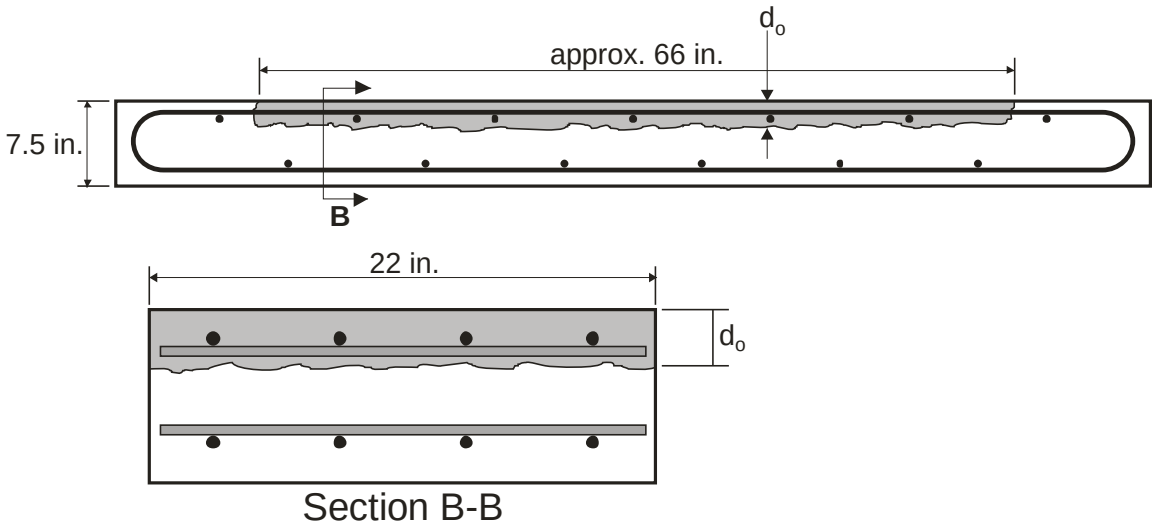

Figure 11: Schematic Detail of LMC Overlay

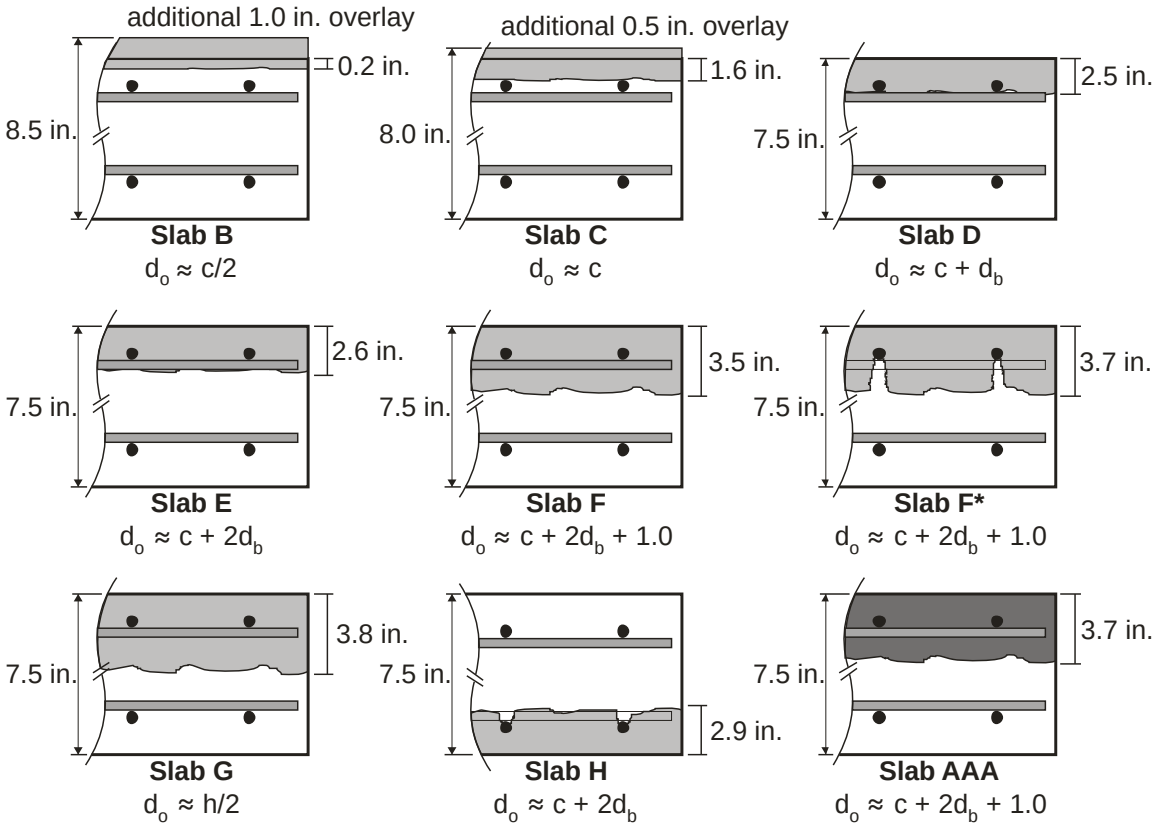

Figure 12: Schematic Details of all Laboratory-cast LMC Slabs

Table 4: Measured Depths of Hydrodemolition

Slab	target depth	measured depths (in.)							
		1	2	3	4	5	6	Average	COV
B	c/2 = 0.75	0.25	0.0	0.0	0.25	0.38	0.25	0.2	0.82
C	c = 1.5	1.50	1.75	1.38	1.25	1.75	1.75	1.6	0.14
D	$c+d_b = 2.2$	2.50	2.50	2.75	2.25	2.00	2.75	2.5	0.12
E	$c+2d_b = 2.8$	2.25	2.50	2.25	3.00	3.25	2.50	2.6	0.16
F	$c+2d_b +1 = 3.8$	3.00	3.25	4.25	3.50	3.50	3.25	3.5	0.12
F*	$c+2d_b +1 = 3.8$	4.25	3.75	3.75	3.50	3.25	3.50	3.7	0.09
G	h/2 = 3.8	3.75	3.75	4.00	3.50	3.50	4.25	3.8	0.08
H	$c+2d_b = 2.8$	2.25	2.75	3.25	2.50	3.00	3.50	2.9	0.16
AAA	$c+2d_b +1 = 3.8$	3.75	4.00	3.50	4.00	3.50	3.50	3.7	0.07
M3	c = 2.0	2.25	2.25	2.00	2.00	1.75	1.88	2.0	0.10
M4	$c+d_b = 2.6$	2.88	3.25	2.50	3.00	2.50	2.75	2.8	0.10

Slabs E and H and F and F* are identical with the exception that the concrete ‘shadows’ beneath the reinforcing steel that result from the HD process have not been removed in Slabs H and F*. Water is directed perpendicular to the slab surface during hydrodemolition, thus concrete in the ‘shadow’ of the top mat of reinforcing steel is not removed. Slab H was tested in the inverted position (i.e. LMC at tension face of slab), representing the behavior of an overlay in the negative moment region of a continuous slab. Finally, Slab AAA is subject to the same HD as Slab F but a standard PennDOT AAA concrete mix is used instead of LMC for the overlay.

3.1.2 Marshall Ave Specimen Details

Figure 13 shows a schematic representation of the decommissioned bridge deck from which the Marshall Ave. slabs were cut. The existing deck was 44 years old at the time of decommissioning. Slabs were cut perpendicular to the longitudinal axis of the bridge (spanning between stringers). However, the one-way flexural direction of this deck was in the longitudinal direction – between floor beams. Thus the slabs, as delivered were tested in their ‘weak’ bending direction. Nonetheless, the slab behavior still provides insight into how overlays applied to older decks may perform in the field.

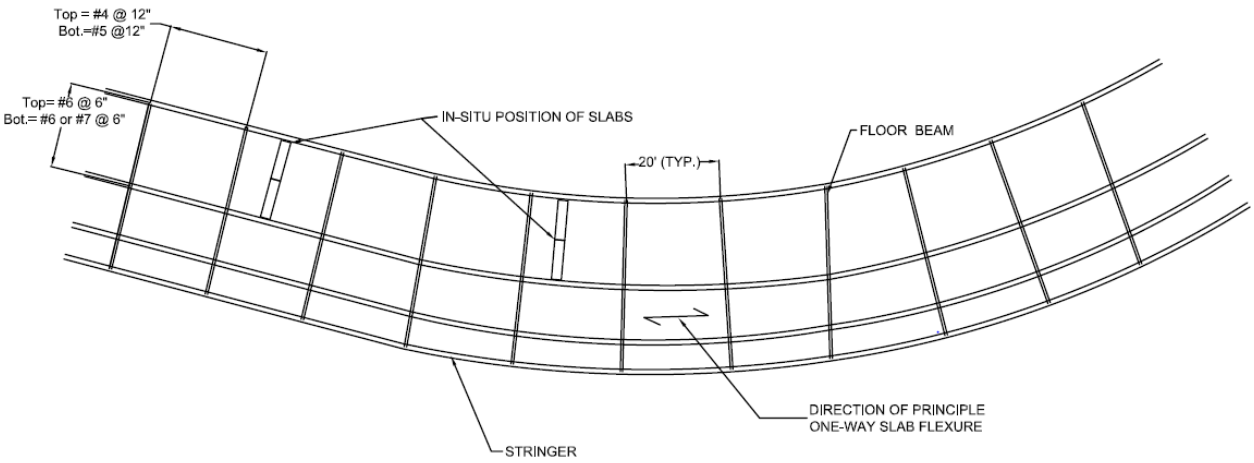

Figure 13: In-Situ Location of Marshall Ave. Slabs

Figure 14 depicts the general geometry of each of the Marshall Ave specimens tested. As evident by the reinforcement bar details, slabs were tested in their inverted position (see Figure 14). This inverted orientation matched the orientation in which the slabs were delivered and was necessary to facilitate testing without requiring additional repairs to the slabs. The position does not change the analysis procedures, only the expected capacities of the specimens (see Section 3.5.2).

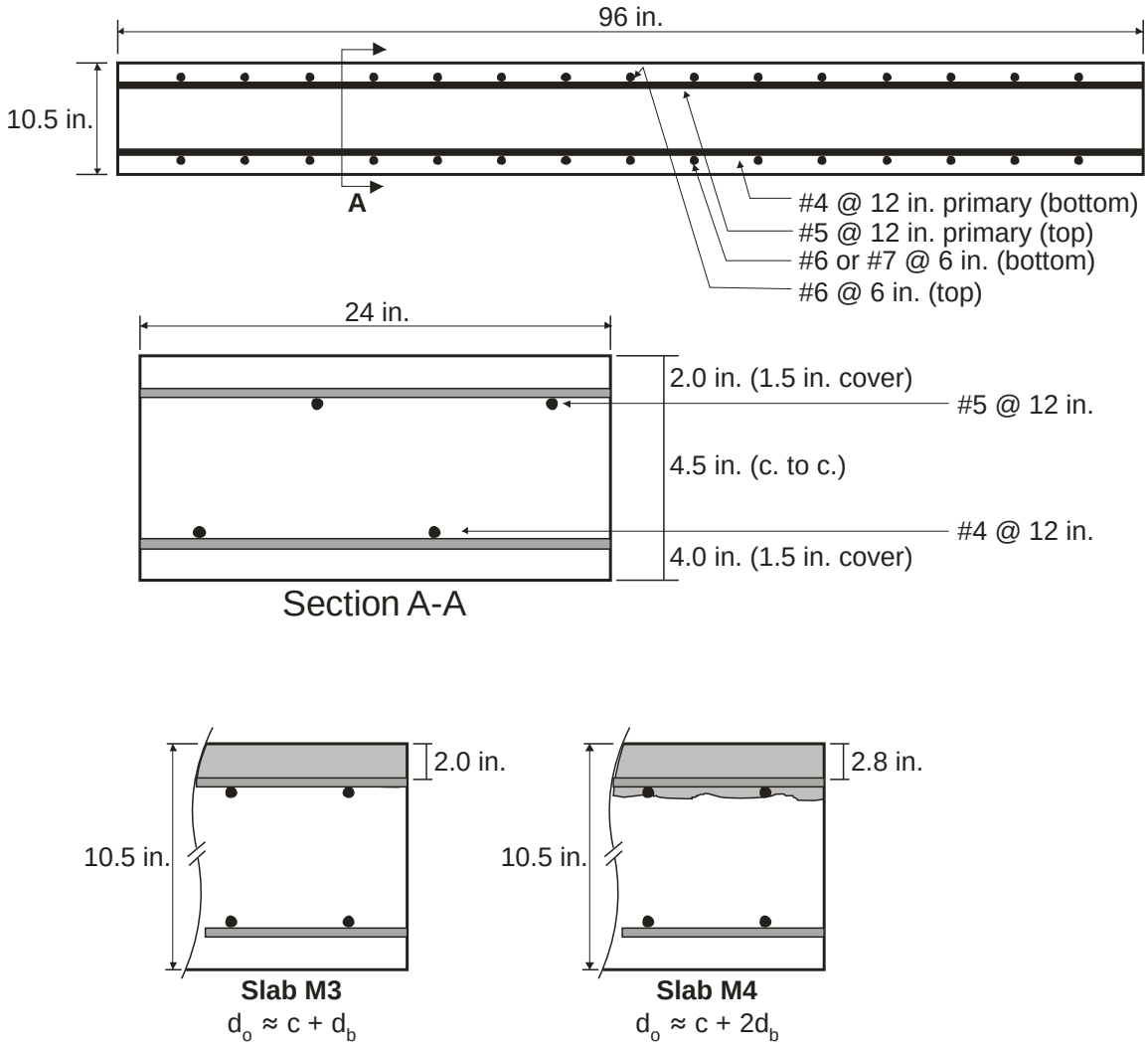

Figure 14: Schematic Details of Marshall Ave. Specimens

Four specimens were tested. Slabs M1 and M2 served as control specimens and thus did not have HD or subsequent overlay applied. Figure 14 and Table 4 shows the measured depths of HD for slabs M3 and M4. Depth measurement techniques were identical to the laboratory specimens.

3.2 SPECIMEN PREPARATION

The laboratory slabs were cast on January 16, 2013. Conventional hydrodemolition – using a manual wand – was carried out by an approved contractor from March 18, 2013 to March 20, 2013 when the laboratory slab concrete was at least 63 days old (Figure 15a). Marshall Ave. slabs M3 and M4, were prepared at the same time.

Following HD, all slabs were stored in a surface-saturated condition until LMC application. During this time 'shadows' – concrete left below exposed reinforcing steel – were removed in all slabs but F* and H using a hand-held electric chipping hammer. All HD surfaces were cleaned of laitance and loose aggregate with water and high pressure air. Immediately prior to LMC application, the interface surface is dried of any standing water although the surface itself remains wetted for the LMC application; this was the typical practice of the contractor and is consistent with recommendations of PennDOT Publication 408.

Finally, the LMC overlays were applied on March 29, 2013 by a PennDOT-approved contractor (Figure 15d). Following LMC application, the slabs were kept under wet burlap for 7 days and then allowed to cure in ambient laboratory conditions.

a) Slabs During Hydrodemolition

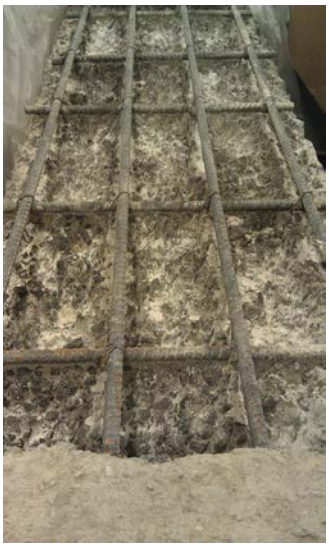

b.) Hydrodemolished Surface Profile

c.) “Shadows” Removed

d) Installing LMC Overlay

Figure 15: HD and LMC Installation Process

3.3 MATERIAL PROPERTIES

3.3.1 Substrate Concrete and Slab AAA Overlay Concrete

A PennDOT-approved AAA mix was provided by local ready-mix supplier for both the laboratory slabs and the overlay for Slab AAA. The mix design reported by the supplier is shown in Table 5. Measured 28-day concrete compression strength (f_c' per ASTM C39), split cylinder tension strength (f_{sp} per ASTM C496) and modulus of rupture (f_r per ASTM C78) are given in Table 6. All cylinders were standard 4 in. (102mm) diameter cylinders and the modulus of rupture specimens were standard 6 in. (152 mm) beams.

2.25 inch (57 mm) diameter cores were taken from Slab A following all testing in order to confirm *in situ* concrete strength. Compressive strength from these cores is also shown in Table 6 and seem to agree well with the 28-day strength.

A rule of thumb is that the direct tension capacity of conventional concrete is approximately $0.70f_{sp}$ and $0.50f_r$. Therefore the direct tension capacity of the concrete in the test specimens is on the order of 320 - 400 psi (2.2-2.8 MPa) ($4\sqrt{f_c}' - 5\sqrt{f_c'}$ in psi units). The recommended value of direct tension strength is typically given as $4\sqrt{f_c}'$ (psi units), in this case, 320 psi (2.2 MPa).

For the Marshall Ave. specimens, the substrate concrete was cored using a 2.25 inch (57 mm) coring bit. Three cores had an average compression strength of 5017 psi (34.6 MPa) with a standard deviation of 714 psi (4.9 MPa). It should be noted that experimental evidence suggests that using cored and small diameter samples typically yields results that are lower and more scattered than *in-situ* strength (Bartlett and Macgregor 1994).

3.3.2 Latex-Modified Overlay Concrete

A PennDOT-approved latex-modified concrete was provided for all overlays. The same batch of LMC was used for both Marshall Ave and laboratory-cast specimens. The mix design reported by the supplier is shown in Table 5. Measured 7 and 28-day concrete compression strength and split cylinder tension strength are given in Table 6. All cylinders were standard 4 in. (102 mm) diameter cylinders.

The LMC was made with Styrofan 1186, an aqueous styrene-butadiene copolymer dispersion manufactured by BASF and pre-qualified under FHWA RD-78-35. This prequalification is considered acceptable per PennDOT Pub. 408 Section 1042.2e.

Table 5: Mix Designs for PennDOT AAA Concrete and LMC Overlay.

<table>
<tr><th></th><th colspan="2">AAA Concrete</th><th colspan="2">LMC Concrete</th></tr>
<tr><td>Supplier</td><td colspan="2">Frank Bryan Concrete</td><td colspan="2">Trumbull</td></tr>
<tr><td></td><td>material</td><td>mix (lbs/yd^3)</td><td>material</td><td>mix (lbs/yd^3)</td></tr>
<tr><td>cement</td><td>Type I/II (Lehigh)</td><td>540</td><td>Type I/II (CEMEX)</td><td>658</td></tr>
<tr><td>pozzolan</td><td>Class C flyash (CEMEX)</td><td>110</td><td>-</td><td>-</td></tr>
<tr><td>coarse aggregate</td><td>#57
(Greer Limestone)
<table><tr><th>screen</th><th>% passing</th></tr><tr><td>1-1/2”</td><td>100</td></tr><tr><td>1”</td><td>99</td></tr><tr><td>1/2"</td><td>46.5</td></tr><tr><td>#4</td><td>2.2</td></tr><tr><td>#8</td><td>1.0</td></tr></table></td><td>1776</td><td>A8
(Allegheny Minerals)
<table><tr><th>screen</th><th>% passing</th></tr><tr><td>1/2”</td><td>100.0</td></tr><tr><td>3/8”</td><td>91.5</td></tr><tr><td>#4</td><td>25.7</td></tr><tr><td>#8</td><td>3.5</td></tr><tr><td>#16</td><td>0.8</td></tr></table></td><td>1070</td></tr>
<tr><td>fine aggregate</td><td>A
(Tri State River Prod.)
<table><tr><th>screen</th><th>% passing</th></tr><tr><td>#4</td><td>99</td></tr><tr><td>#8</td><td>83</td></tr><tr><td>#16</td><td>61</td></tr><tr><td>#30</td><td>41</td></tr><tr><td>#50</td><td>14</td></tr><tr><td>#100</td><td>3</td></tr></table></td><td>1172</td><td>A
(Hanson Agg.)
<table><tr><th>screen</th><th>% passing</th></tr><tr><td>3/8”</td><td>100.0</td></tr><tr><td>#4</td><td>98.6</td></tr><tr><td>#8</td><td>83.5</td></tr><tr><td>#16</td><td>69.1</td></tr><tr><td>#30</td><td>55.6</td></tr><tr><td>#50</td><td>20.9</td></tr><tr><td>#100</td><td>5.3</td></tr></table></td><td>1706</td></tr>
<tr><td>mix water</td><td>-</td><td>267</td><td>-</td><td>124</td></tr>
<tr><td>admixture water</td><td>-</td><td>-</td><td>-</td><td>109</td></tr>
<tr><td>AEA</td><td>AIR-260 (SIKA)</td><td>1 oz/cwt</td><td>-</td><td>-</td></tr>
<tr><td>RR</td><td>Plastocrete 10N (SIKA)</td><td>3.5 oz/cwt</td><td>-</td><td>-</td></tr>
<tr><td>latex</td><td>-</td><td>-</td><td>Styrofan 1186 (BASF)</td><td>210</td></tr>
<tr><td>w/c</td><td>-</td><td>0.410</td><td>-</td><td>0.354</td></tr>
<tr><td>unit weight</td><td>-</td><td>143</td><td>-</td><td>140</td></tr>
<tr><td>reported trial mix strength</td><td>7 day
28 day</td><td>4776 psi
6559 psi</td><td>5 day
28 day</td><td>4622 psi
6481 psi</td></tr>
</table>

Table 6: Concrete Material Properties

age (days)	ASTM C39 compression tests			ASTM C496 split cylinder tests			ASTM C78 modulus of rupture		
	n	f_c (psi)	COV	n	f_{sp} (psi)	COV	n	f_r (psi)	COV
	AAA substrate slab concrete								
28	3	6501	3.4%	3	$453 = 5.6\sqrt{f_c'}$	13.1%	3	$790 = 9.8\sqrt{f_c'}$	5.6%
132	3 cores	6647	8.4%	-	-	-	-	-	-
	latex-modified concrete overlay								
7	3	4718	0.7%	-	-	-	-	-	-
28	3	6568	4.4%	3	$641 = 7.9\sqrt{f_c'}$	11.7%	-	-	-
	AAA overlay (Slab AAA only)								
28	3	4676	5.2%	3	$441 = 6.4\sqrt{f_c'}$	6.4%	-	-	-

3.3.3 Reinforcing Steel

Reinforcing steel exhibited different material properties among the laboratory and field slabs. For the laboratory slabs, the #5 A615 reinforcing steel had experimentally determined yield and tensile strengths of 67.8 ksi (467 MPa) and 107.9 ksi (744 MPa), respectively. Reinforcing steel from the field slabs was recovered from an untested slab; yield and ultimate strength were experimentally determined to be 43.0 ksi (296 MPa) and 66.7 ksi (460 MPa), respectively.

3.4 TEST SET-UP AND INSTRUMENTATION

Laboratory and Marshall Ave specimens were tested over span lengths (L) of 84 and 72 inches (2134 and 1829 mm), respectively (see Figure 16). The selection of an 84 in. (2134 mm) simple span is based on a slab-on-steel girder bridge having a girder spacing S = 8 ft (2.44 m) and a top flange dimension b_f = 12 in. (305 mm). In such a case, the clear span of the slab is 84 in.

(2134 mm). A shorter span length was selected for the Marshall Ave. specimens in order to avoid placing existing damage directly under the supports. In all slabs but H, the LMC overlay is placed in compression representing positive flexure typical of a slab spanning between girders. Slab H was tested in the inverted position (i.e. LMC at tension face of slab), representing the behavior of an overlay in the negative moment region of a continuous slab. Support points were full-width 4 in. (102mm) diameter rockers transitioned to the slab through 3/8 in. (10 mm) steel plates. The load location was a 2 in. (50 mm) wide by 1/2 in. (13 mm) deep neoprene pad. Load was applied through a full-width spreader beam and single 60 kip (267 kN) hydraulic ram with a ball joint between the ram and spreader beam. Applied load is calculated from hydraulic pressure with a precision of 72 pounds (320 N). Displacement at mid-span is measured manually with a precision of 1/32 in. (0.8 mm). The combined 130 pound (578 N) weight of the ball joint and spreader beam is added to all recorded applied loads.

DEMEC targets having an 8 in. (203 mm) gauge length are applied at mid-span on both sides of the slab. The DEMEC instrument used (Figure 16c) has a resolution of 8 microstrain. Target locations vary vertically for each slab but were selected to capture at least the following:

- centroid of tensile steel (1.82 in. (46.2 mm) above soffit for laboratory specimens)
- immediately above and below the LMC interface
- as near to the extreme compression fiber as possible (1/2 in. (13mm) below top of slab)
- a fifth location was selected to provide good data distribution

Load was applied to the laboratory slabs in increments of approximately 1000 pounds (4.45 kN); at each step a complete set of instrument readings was recorded. Load increments were reduced to 333 pounds (1.48 kN) for the Marshall Ave. specimens. Reducing the load increment allowed for similar data resolution for the field specimens, which had lower capacities than

laboratory specimens. Following yield of the slab, instruments were recorded at displacement increments not exceeding 1/16 in (1.6 mm).

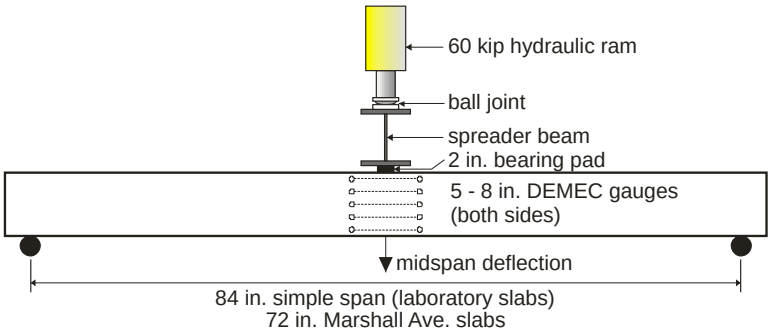

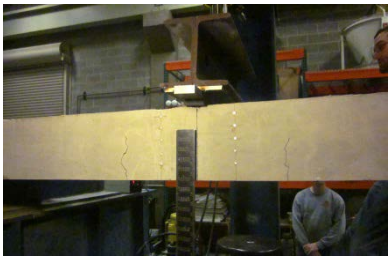

b) DEMEC and Vertical deflection instrumentation

a) Test Set-up (Slab A shown)

c) DEMEC Reader (wexham-developments.co.uk)

Figure 16: Test Set-Up and Instrumentation

3.5 PREDICTIONS OF SLAB BEHAVIOR

3.5.1 Laboratory Slab Predictions

In order to verify the laboratory control slab behavior and establish a baseline against which to compare test data, a fiber-element model of the control test slab was analyzed. This, and all successive analysis were conducted using the program RESPONSE (Bentz 2000), a fiber-element plane-sections analysis tool that incorporates the modified compression field theory. RESPONSE is well established in both the research and consulting communities.

Figure 17 shows the moment-curvature response predicted for the control slab A calculated using measured material properties and as-tested dimensions. Also shown are AASHTO slab design moments determined based on the AASHTO 'strip method' calculations (AASHTO LRFD §4.6.2.1.1 as tabulated in AASHTO Appendix A4). The positive live load design moment for S = 8 ft (2.44 m) is M_{LL} = 5.69 kft/ft (25.31 kNm/m). Dead load moment for the 7.5 in. (191 mm) thick slab, M_{DL} = 0.75 kft/ft (3.34 kNm/m) is added to this value. These values are multiplied by 22/12 to account for the 22 in. (559 mm) specimen width. The moments shown are based on the AASHTO SERVICE I and STRENGTH I load combinations as summarized in Table 7.

Table 7: Laboratory Slab Design Moments.

'strip method' moments (AASHTO§ 4.6.2.1.1)		22 in. wide specimen moments	
		SERVICE I	STRENGTH I
M_{LL}	M_{DL}	$(22/12)(M_{DL} + M_{LL})$	$(22/12)(1.25M_{DL} + (1.33 \times 1.75M_{LL})$
5.69 kft/ft	0.75 kft/ft	11.8 kft	26.0 kft

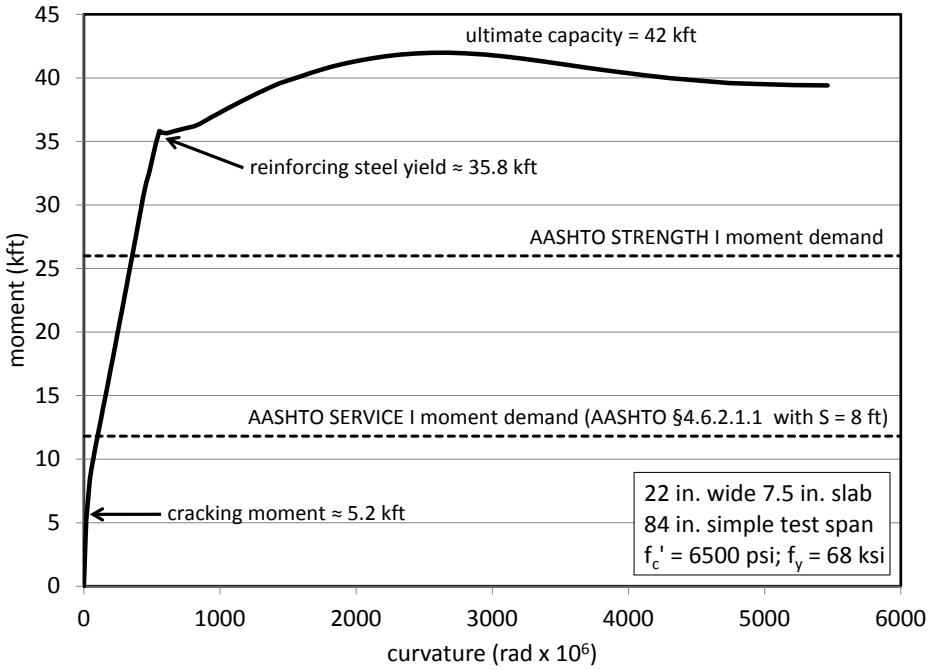

Figure 17: Predicted Moment-Curvature Behavior of Laboratory Control Slab

Figure 18 presents the slab moment capacity with decreasing concrete depth as concrete is removed from the top of the slab; essentially the capacity of the slab as it is subject to HD. The data shown represents a series of plane sections analyses conducting using program RESPONSE. The slab depth is measured from the soffit. Once the slab depth falls below the layer of the top reinforcing steel (at 6.2 in. (157 mm)), the contribution of the top steel is neglected (hence the step in the ultimate capacity curve). In terms of capacity, Figure 18 demonstrates that a slab of 6.0 in. (152 mm) is required to resist the factored load demand (STRENGTH I) while a 4 in.(102 mm) slab is adequate to resist the nominal demand (SERVICE I). The predicted ultimate deflection for a 7.5 in.(191 mm) slab is s/225; this falls to s/112 and s/77 for the slabs having a thickness of 6 and 4 in.(152 and 102 mm), respectively. The slab span is S = 84 in. (2134 mm).

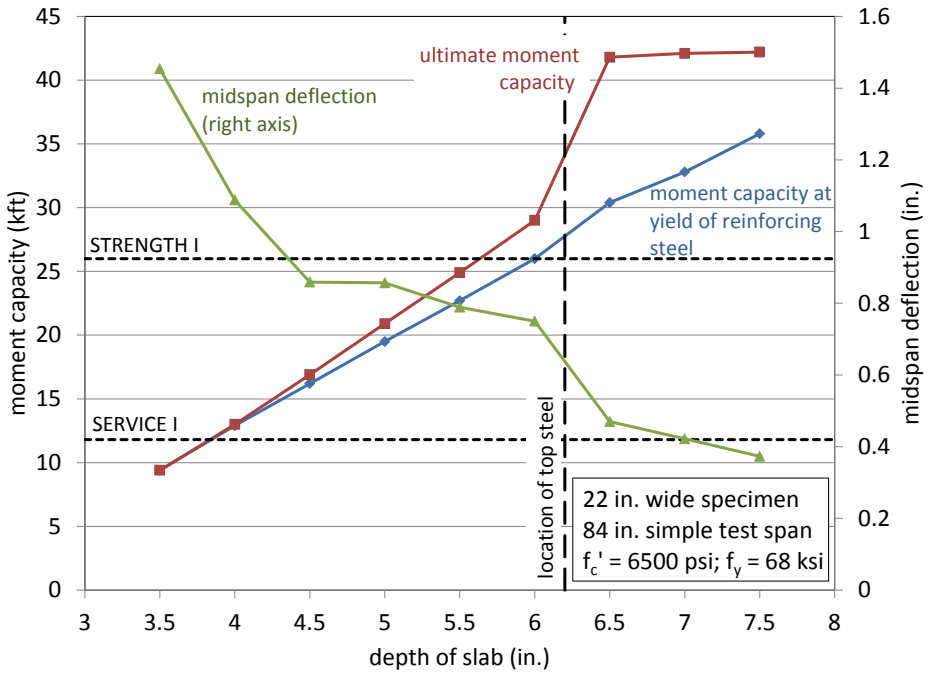

Figure 18: Predictions of Laboratory Slab Behavior if LMC does not contribute to Slab Capacity

3.5.2 Marshall Ave. Slab Predictions

A RESPONSE model was also used to establish a baseline for the Marshall Ave. specimens. The moment curvature response is shown in Figure 19. This model was generated for measured material properties and geometry of the cross-section depicted in Figure 13. In these very lightly reinforced slabs, the pre-cracking behavior is not noticeable, since steel yields at approximately the same time as cracking occurs. Additionally, since the slabs were cut transverse to their principle directions, AASHTO design moments are not applicable.

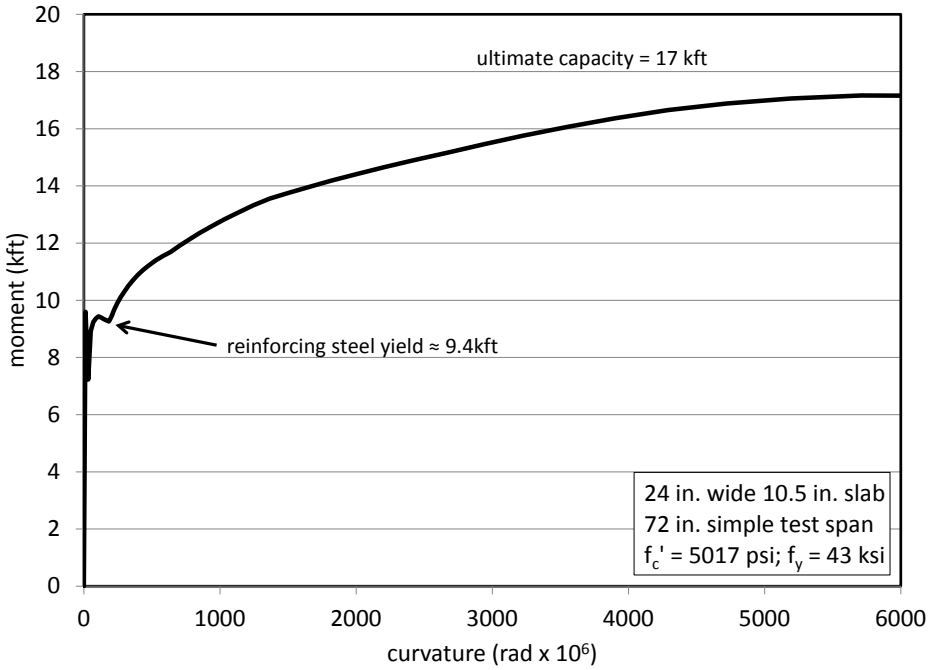

Figure 19: Predicted Moment-Curvature Response of Marshall Ave. Specimens (No Overlay)

Figure 20 shows the moment capacity and deflection predictions of Marshall Ave. specimens assuming that the overlay had no contribution to the slab capacity. Once the depth of hydrodemolition was beyond the depth of the top mat of reinforcement steel, the top steel was neglected. Moment capacities exhibited similar behavior in both Marshall Ave. and laboratory specimens. Marshall Ave. slabs exhibited different deflection predictions when compared to the laboratory predictions. Deflections increase as depth is decreased to a point at which the ultimate capacity of the slab is no longer high enough to result in large deflections at which point, ultimate deflections decrease as the slab depth is reduced further.

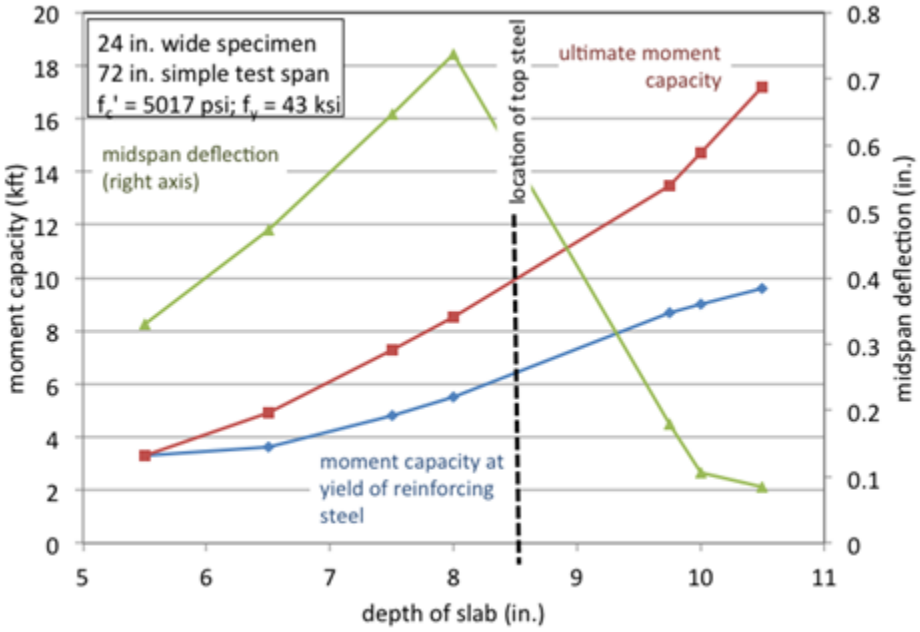

Figure 20: Predictions of Marshall Ave. Slab Behavior if LMC does not Contribute to Slab Capacity

4.0 RESULTS

Tables 8 and 9 summarize key results from the laboratory and Marshall Ave. specimens, respectively, while Figures 22 through 34 provide details of each slab test. Due to significant existing cracking in slab M2, reliable strain profiles and moment curvature could not be obtained; therefore only observed loads are reported in Table 9. The data shown in Figures 22 to 34 is described as follows:

Figures a show the moment-curvature (M-φ) diagrams; both experimental (solid line) and analytical (dashed line) predictions are presented. Moment is the applied moment, neglecting self-weight of the slab, and is calculated as: M = PL/4. The curvature is calculated from the individual strain profiles (see below) by dividing the absolute difference in strain between the top- and bottom-most DEMEC gages by the vertical distance between the gage lines. The analytical curves are generated using RESPONSE as described above (see Figures 17 and 19) using the geometry and material properties of each slab.

Figures b show the strain profiles determined directly from DEMEC readings plotted at their appropriate vertical locations. For clarity, profiles at all loading intervals are not shown. Although DEMEC readings were recorded from both sides of each test slab, results from only one side are shown. The results shown are from the side capturing uniform cracking. The location of the LMC interface is also shown in each instance.

DEMEC gages report the *average strain* over their gage length; 8 in. in this case. It is expected that multiple cracks will intersect the gage lengths and the strain reading is therefore essentially the sum of the crack widths since concrete strain between cracks is negligible. In cases

were a crack passes from outside the gage length to inside the gage length between gages – as shown in the circled region of Figure 21a – the DEMEC reading between adjacent gages is affected as shown in Figure 21b. In the case shown in Figure 21, three cracks are included in the top four gages. The right-most crack passes outside the gage at the bottom DEMEC gage; the associated crack width (strain) is therefore not captured in the reading and the apparent bottom strain falls. In this case, the curvature is calculated over the linear section from the top gage to the fourth gage.

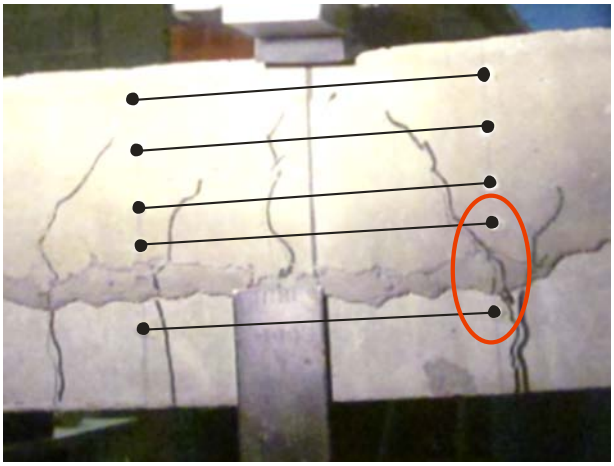

a) Crack pattern on Slab AAA (gages enhanced)

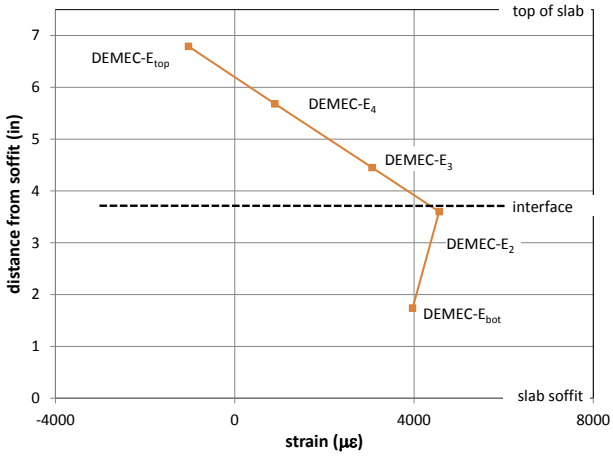

b) Strain Profile of Slab AAA (at 35.4 k-ft)

Figure 21: Example of the Effect of Crack Location on Strain Profiles (Slab AAA shown)

Figures c show the location of the neutral axis derived from the slope of the strain profiles. This calculation was made by assuming linearity between two points on the strain profile and using a linear equation to calculate the y-axis intercept. In all cases, the y-axis is given as the distance from the soffit. The location of the LMC interface is also shown in each instance.

Figures d, e and f show photographs at key milestones in the load application process: reinforcement yield, final DEMEC reading (DEMEC gages have a limit of about 15000 με), and ultimate load, respectively.

Table 8: Summary of Key Test Results-Laboratory Specimens

	A	B	C	D	E	F	F*	G	H	AAA
depth of slab (in.)	7.5	8.5	8.0	7.5	7.5	7.5	7.5	7.5	7.5	7.5
depth of overlay (in)	none	1.2	2.1	2.5	2.6	3.5	3.7	3.8	2.9	3.7
load at first crack (kips)	5.08	7.13	3.10	5.15	5.13	4.11	5.13	5.13	6.14	-
moment at first crack (kft)	8.89	12.47	5.42	9.01	8.97	7.19	8.97	8.97	10.74	-
load at reinforcing yield (kips)	18.19	27.13	23.15	20.18	20.18	20.08	20.13	20.23	20.15	20.15
moment at reinforcing yield (kft)	31.83	47.47	40.51	35.31	35.31	35.14	35.22	35.40	35.26	35.26
ratio yield capacity to Slab A	-	1.49 1.16[1]	1.27 1.12[1]	1.11	1.11	1.10	1.11	1.11	-	1.11
deflection at reinforcing yield (in.)	0.375	0.375	0.343	0.406	0.406	0.406	0.406	0.406	0.343	0.469
curvature at reinforcing yield (rad/in^6)	651	572	571	640	806	622	845	600	565	537
ultimate load (kips)	28.03	39.38	34.13	30.21	29.31	29.17	28.23	31.13	29.24	25.19
ultimate moment (kipft)	49.05	68.91	59.72	52.86	51.29	51.04	49.40	54.47	51.17	44.08
ratio ultimate capacity to Slab A	-	1.40 1.09[1]	1.22 1.07[1]	1.08	1.05	1.04	1.01	1.11	-	0.90
deflection at ultimate load (in.)	-	3.50	2.125	1.81	2.56	2.81	2.5	3.00	2.00	2.25
failure mode	flexural	flexural	flexural	flexural	flexural	flexural	flexural	flexural	flexural	flexural

[1] value normalized to 7.5 in. slab depth; i.e.: Slab B ratio multiplied by $(7.5/8.5)^2$ and SlabC by $(7.5/8.0)^2$

Table 9: Summary of Key Test Results - Marshall Ave. Specimens

	M1	M2	M3	M4
depth of slab (in.)	10.5	10.5	10.5	10.5
depth of overlay (in)	none	none	2.0	2.8
load at first crack (kips)	existing cracking indicating that service loads had exceeded cracking capacity			
moment at first crack (kft)				
load at reinforcing yield (kips)	7.15	7.84	9.51	9.50
moment at reinforcing yield (kft)	10.73	11.76	14.27	14.25
deflection at reinforcing yield (in.)	0.031	0.094	0.188	0.094
curvature at reinforcing yield (rad/in^6)	37.0	n.a.	374.5	376.3
ultimate load (kips)	14.13	14.20	15.13	17.90
ultimate moment (kipft)	21.20	21.30	22.70	26.85
deflection at ultimate load (in.)	3.25	3.00	3.50	4.75
failure mode	flexural	flexural	flexural	flexural

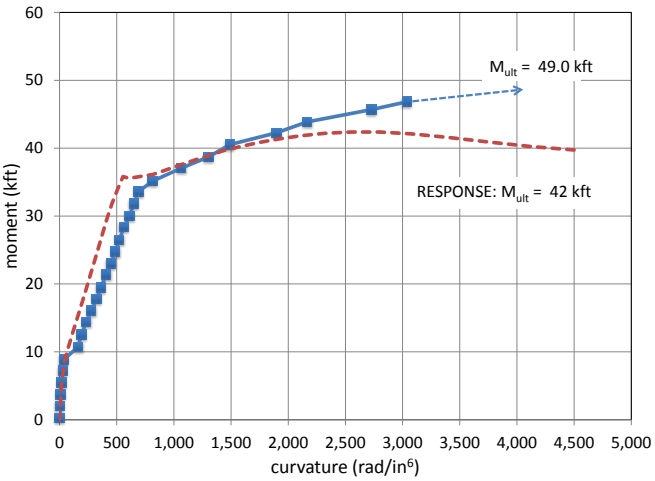

a) Moment-Curvature Plot

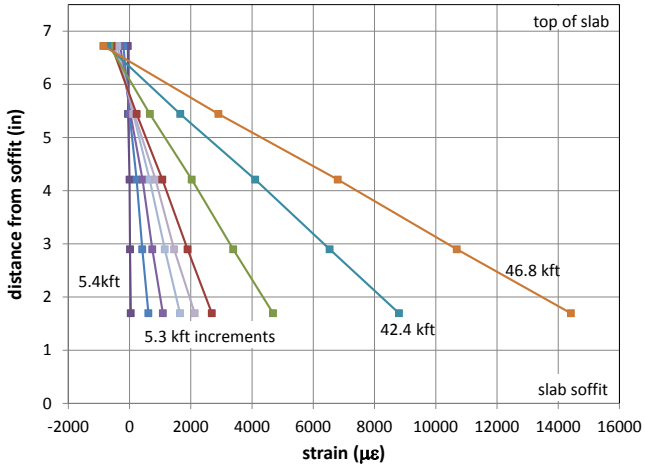

b) Strain Profiles

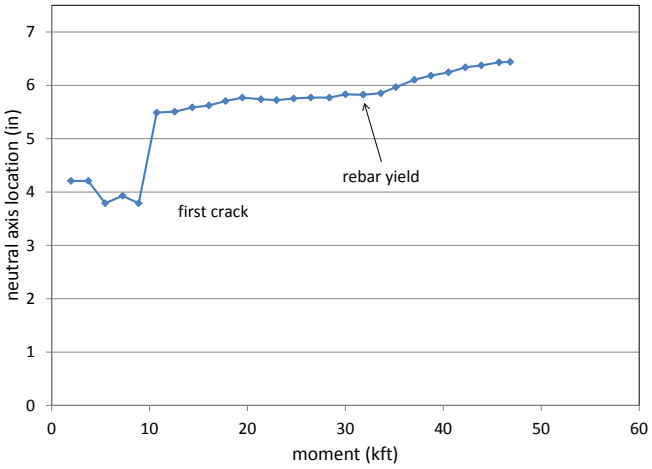

c) Location of Neutral Axis

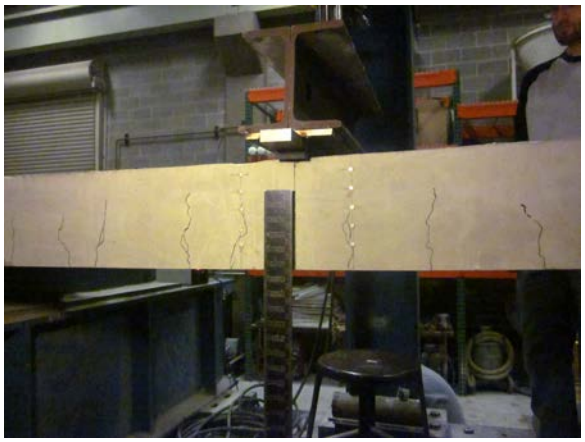

d) Reinforcement Yield (31.8 kipft)

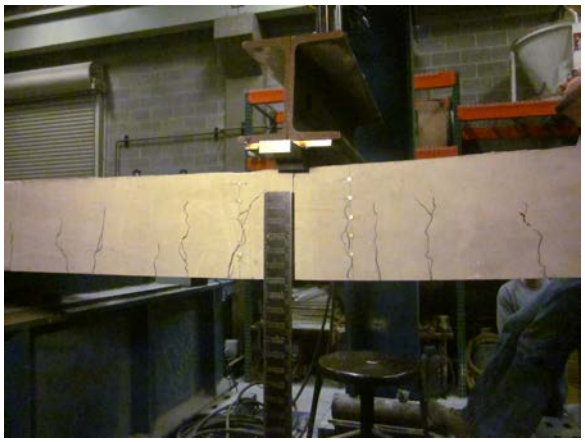

e) Final DEMEC Reading (46.8 kipft)

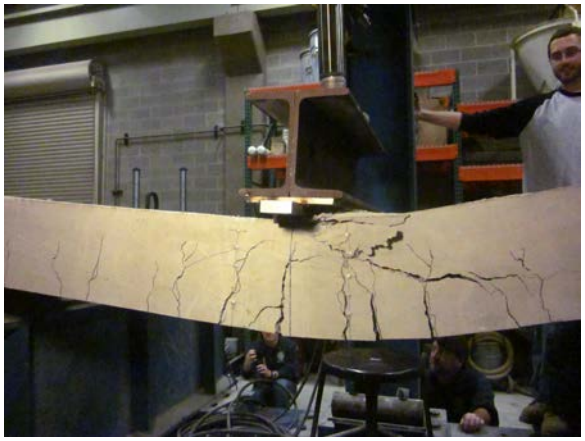

f) Ultimate Load (49.0 kipft)

Figure 22: Slab A Results

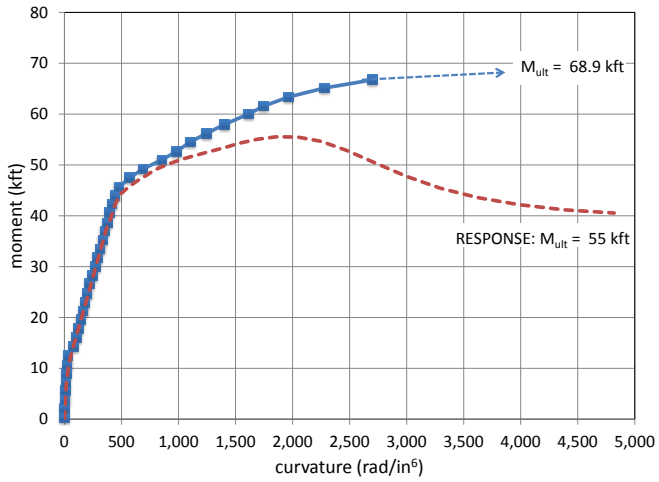

a) Moment-Curvature Plot

d) Reinforcement Yield (47.5 kipft)

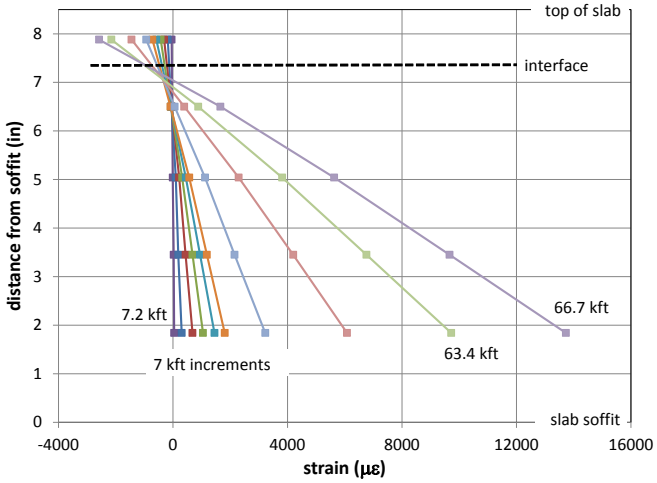

b) Strain Profiles

e) Final DEMEC Reading (66.7 kipft)

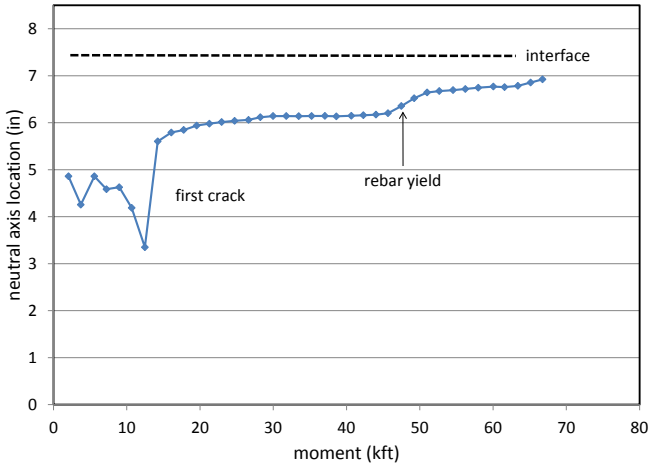

c) Location of Neutral Axis

f) Ultimate Load (68.9 kipft)

Figure 23: Slab B Results

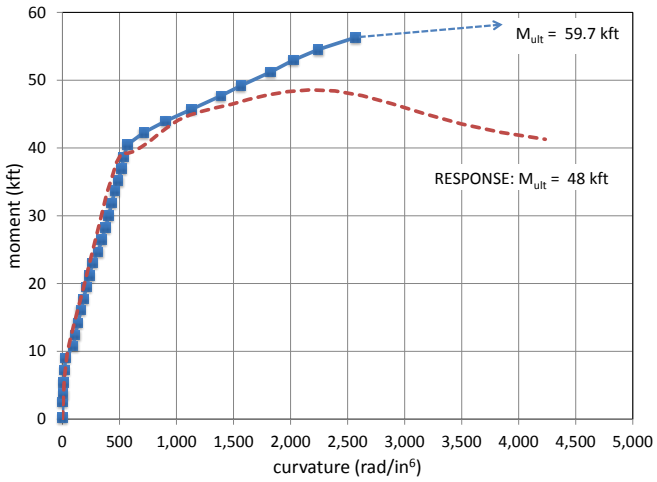

a) Moment-Curvature Plot

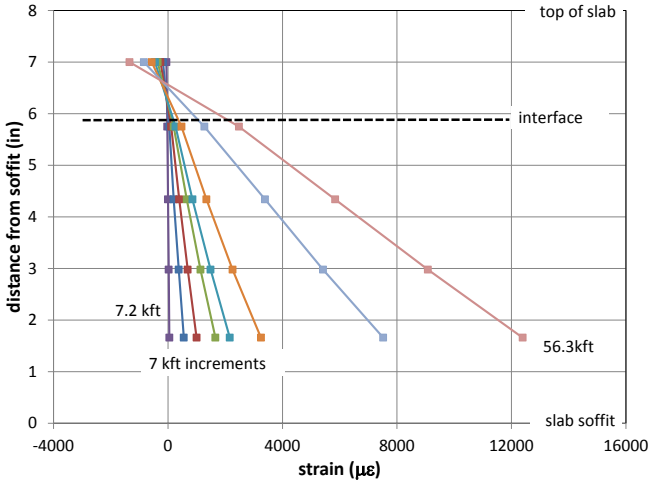

b) Strain Profiles

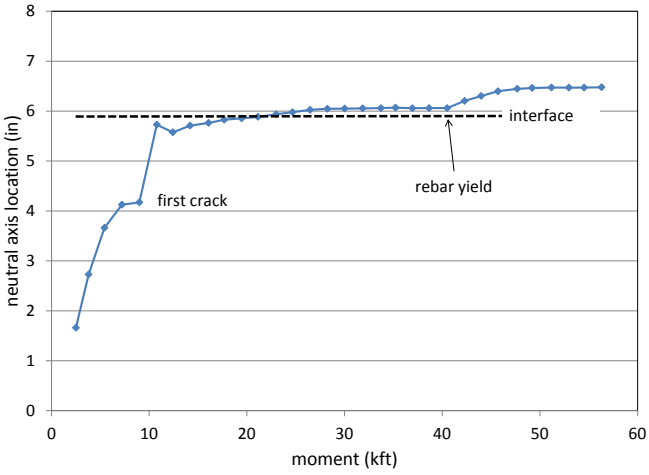

c) Location of Neutral Axis

d) Reinforcement Yield (40.5 kipft)

e) Final DEMEC Reading (56.3 kipft)

f) Ultimate Load (59.7 kipft)

Figure 24: Slab C Results

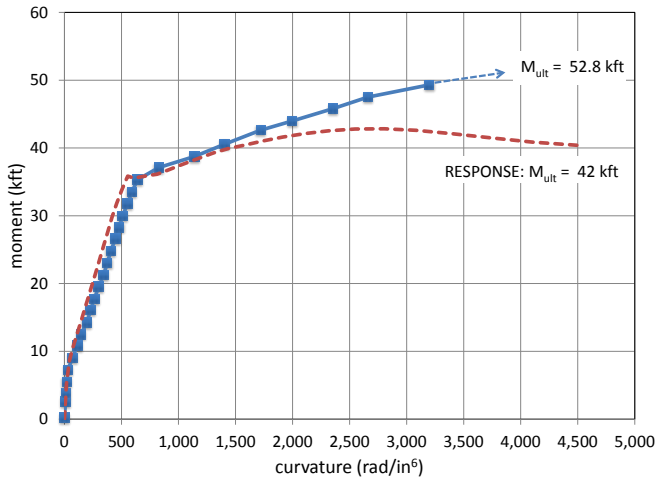

a) Moment-Curvature Plot

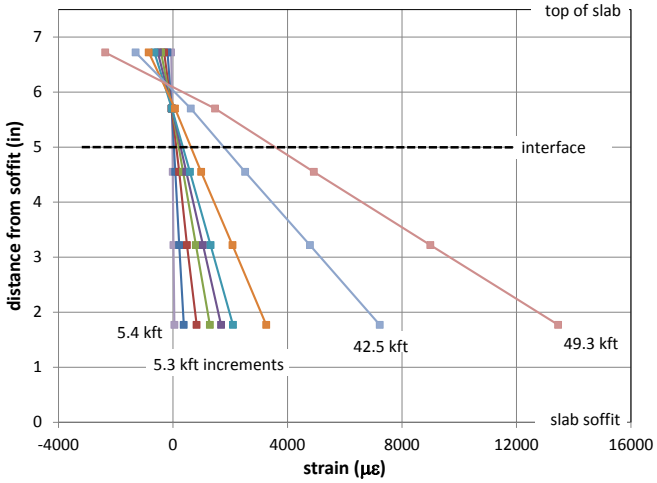

b) Strain Profiles

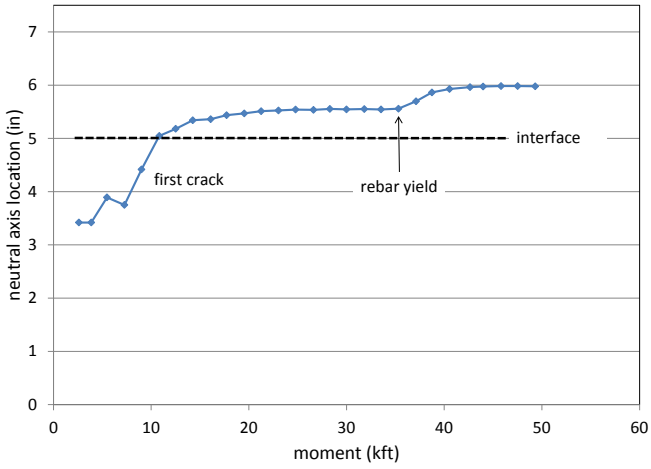

c) Location of Neutral Axis

d) Reinforcement Yield (35.3 kipft)

e) Final DEMEC Reading (49.3 kipft)

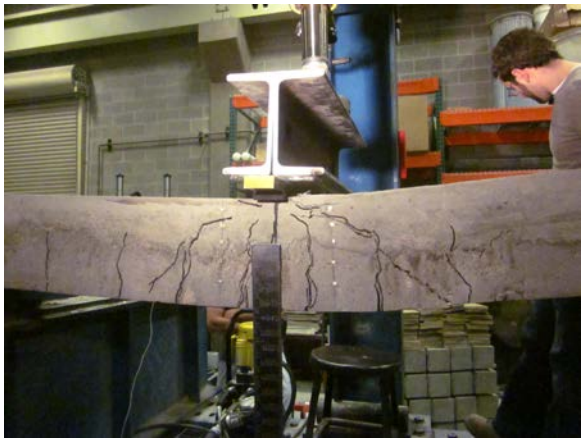

f) Ultimate Load (52.8 kipft)

Figure 25: Slab D Results

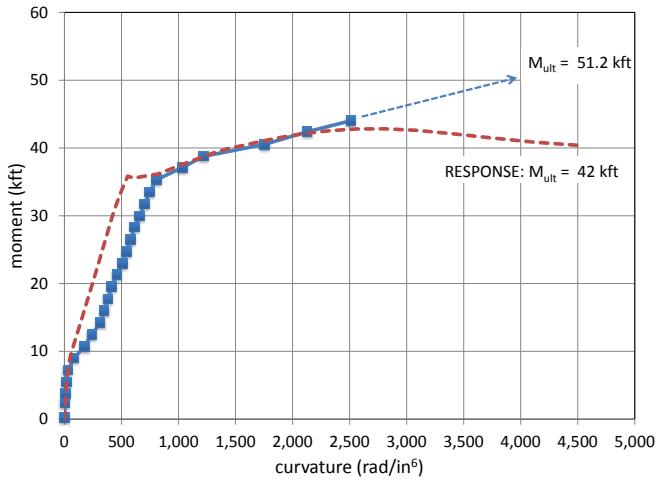

a) Moment-Curvature Plot

d) Reinforcement Yield (35.3 kipft)

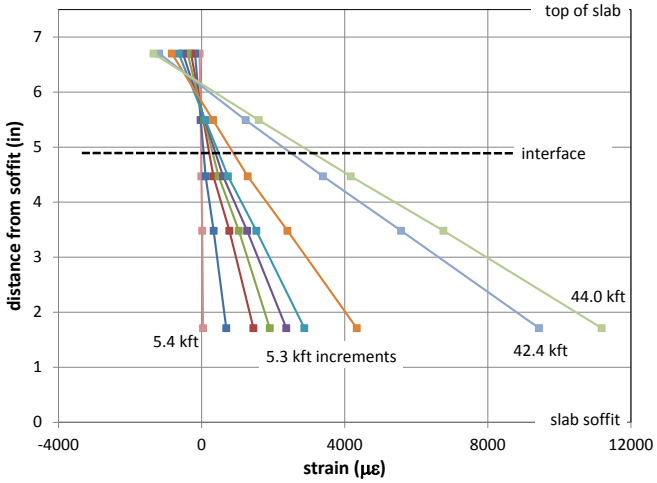

b) Strain Profiles

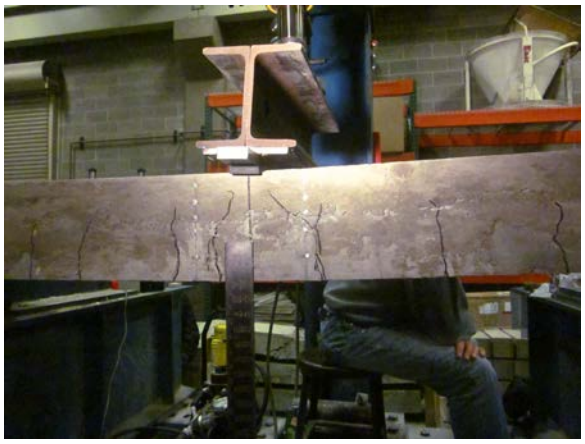

e) Final DEMEC Reading (44.0 kipft)

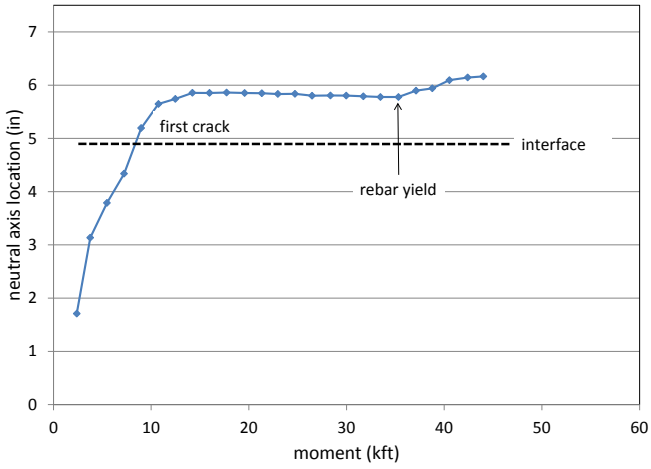

c) Location of Neutral Axis

f) Ultimate Load (51.2 kipft)

Figure 26: Slab E Results

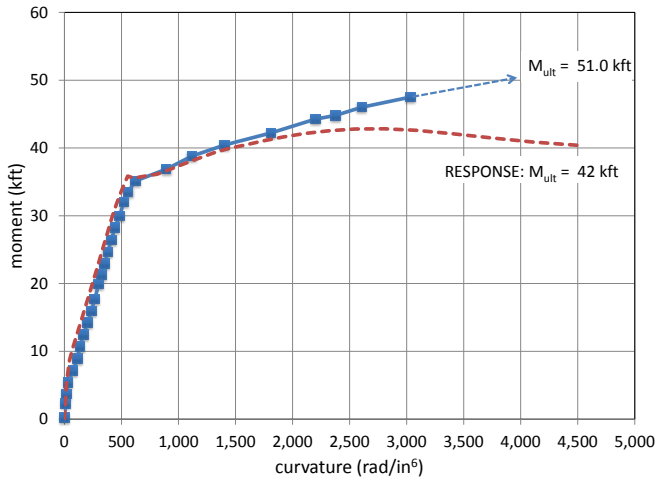

a) Moment-Curvature Plot

d) Reinforcement Yield (35.1 kipft)

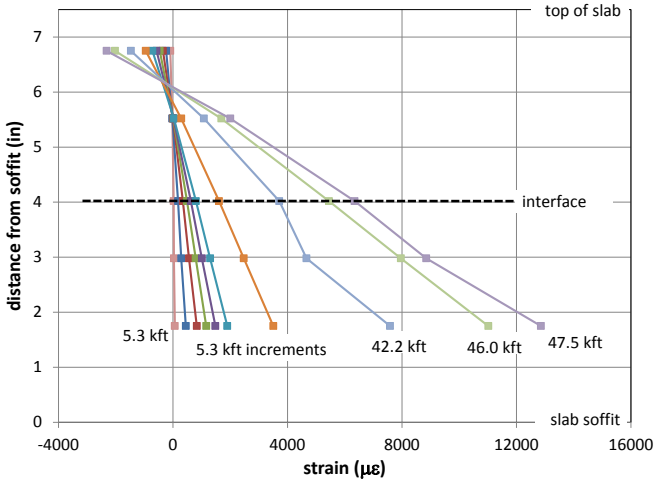

b) Strain Profiles

e) Final DEMEC Reading (47.5 kipft)

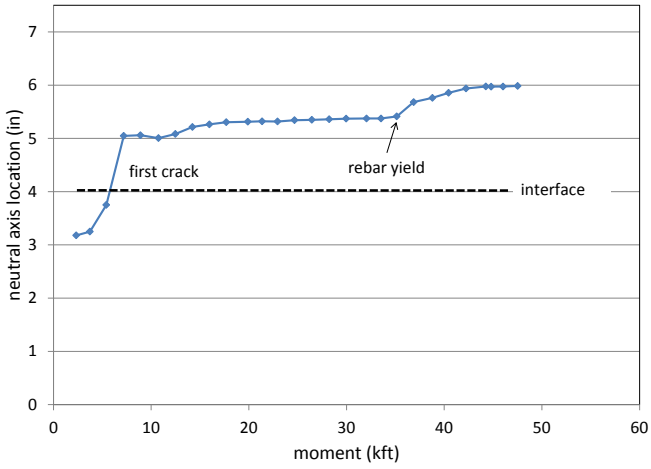

c) Location of Neutral Axis

f) Ultimate Load (51.0 kipft)

Figure 27: Slab F Results

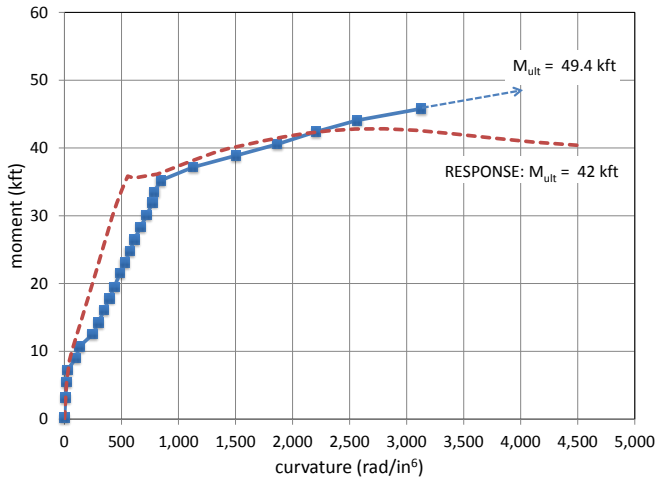

a) Moment-Curvature Plot

d) Reinforcement Yield (35.2 kipft)

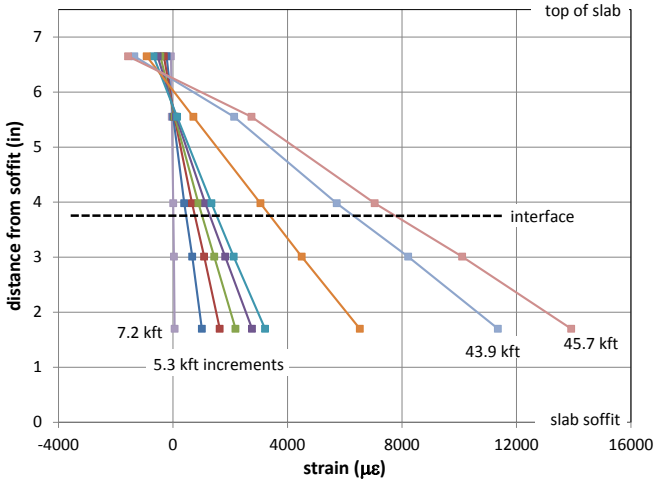

b) Strain Profiles

e) Final DEMEC Reading (45.7 kipft)

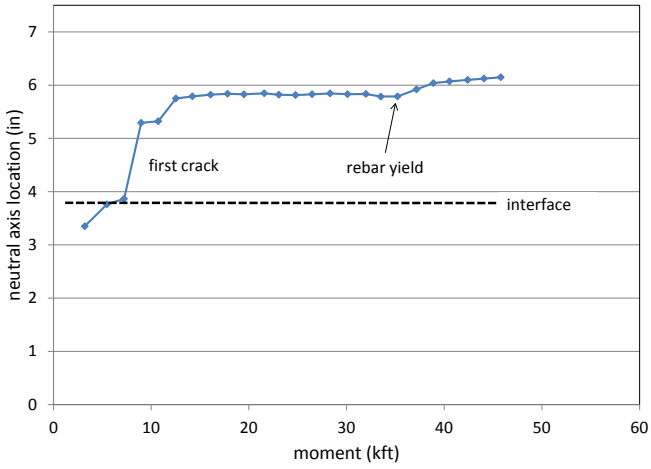

c) Location of Neutral Axis

f) Ultimate Load (49.4 kipft)

Figure 28: Slab F* Results

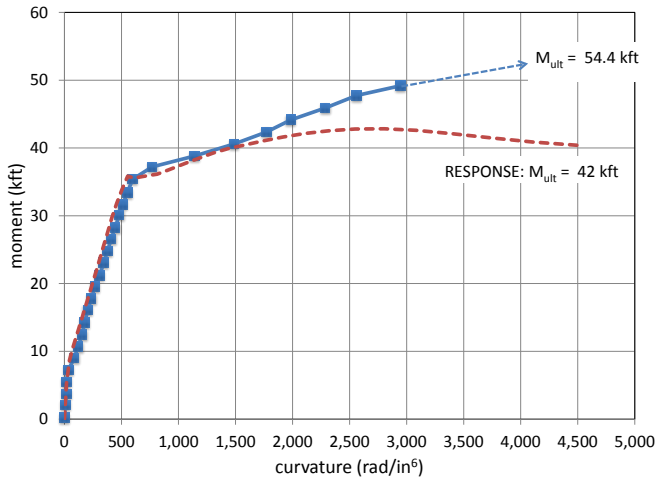

a) Moment-Curvature Plot

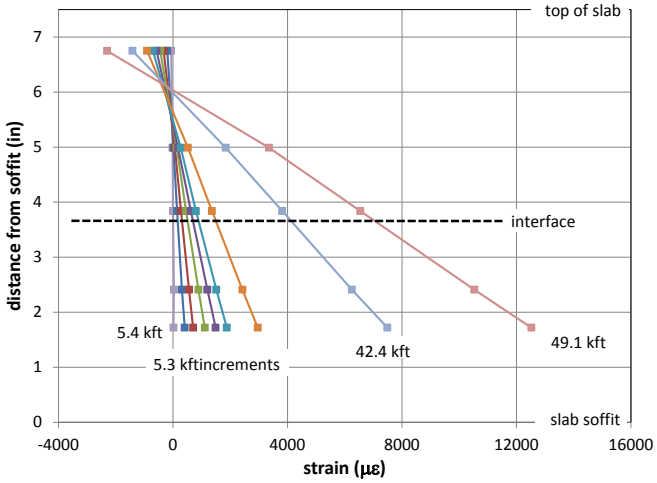

b) Strain Profiles

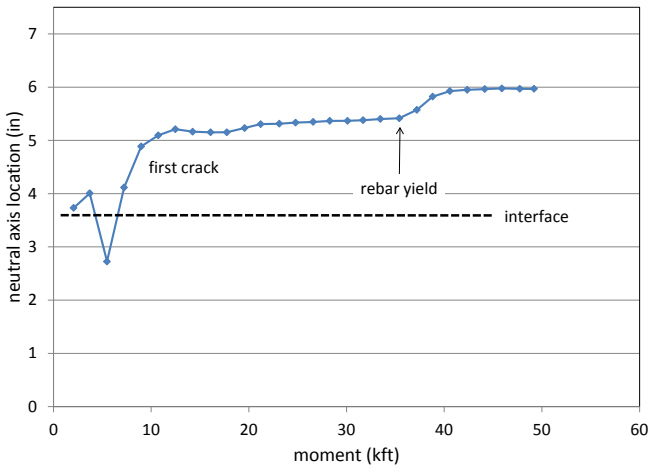

c) Location of Neutral Axis

d) Reinforcement Yield (35.4 kipft)

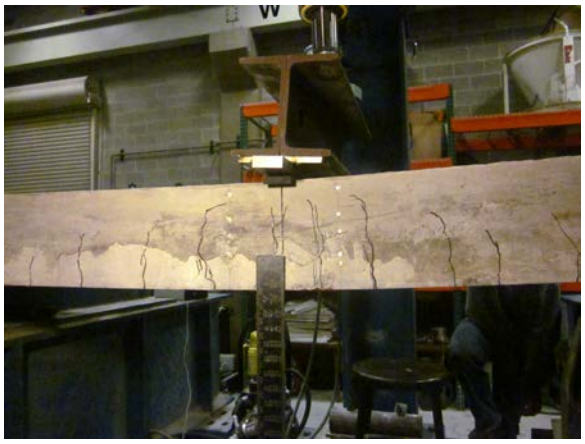

e) Final DEMEC Reading (49.1 kipft)

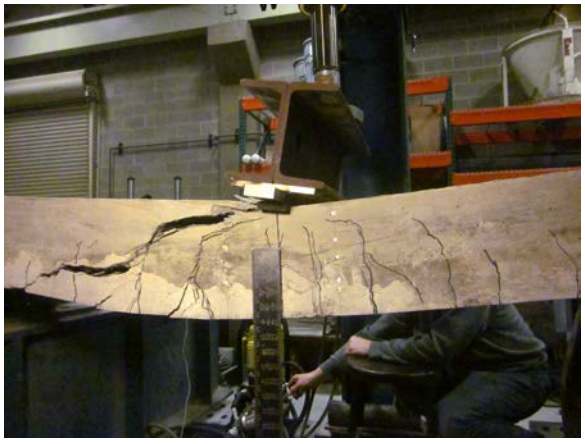

f) Ultimate Load (54.4 kipft)

Figure 29: Slab G Results

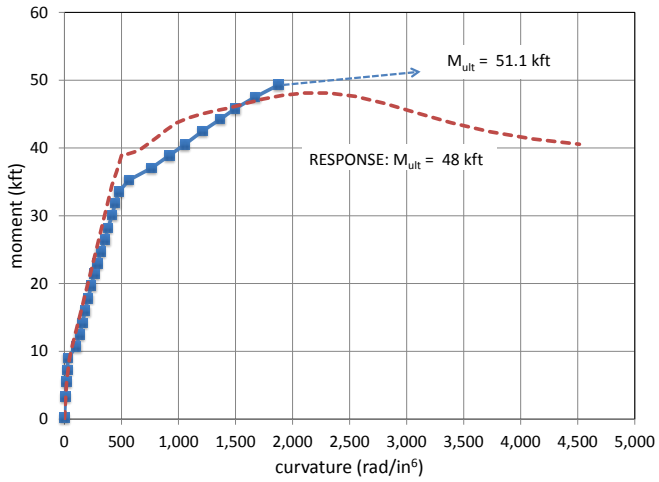

a) Moment-Curvature Plot

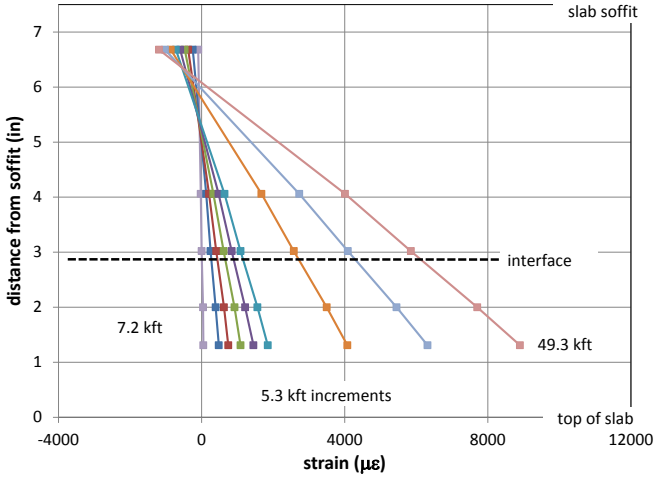

b) Strain Profiles

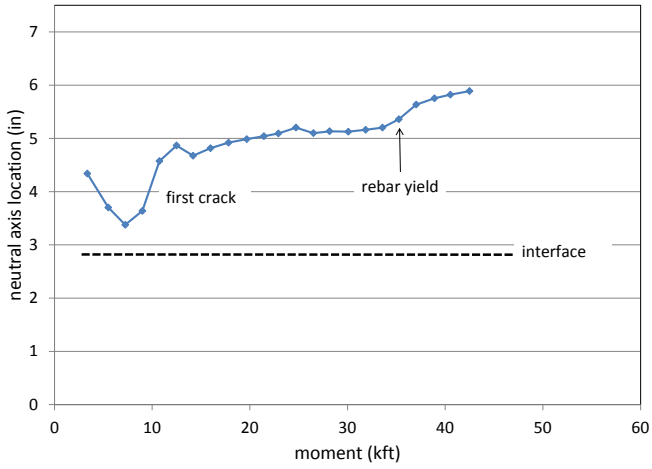

c) Location of Neutral Axis

d) Reinforcement Yield (35.3 kipft)

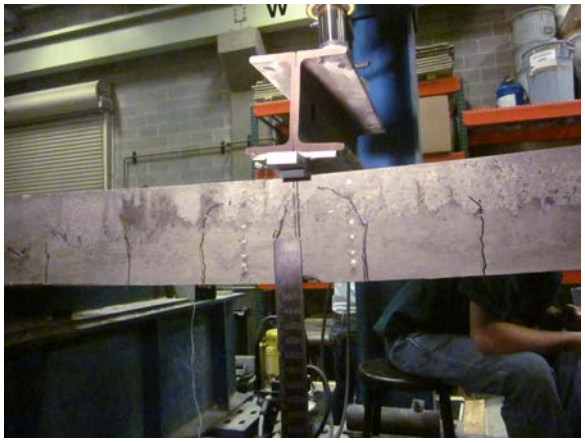

e) Final DEMEC Reading (49.3 kipft)

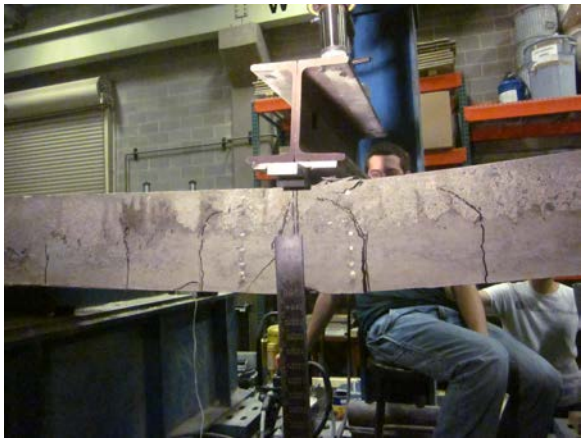

f) Ultimate Load (51.1 kipft)

Figure 30: Slab H Results

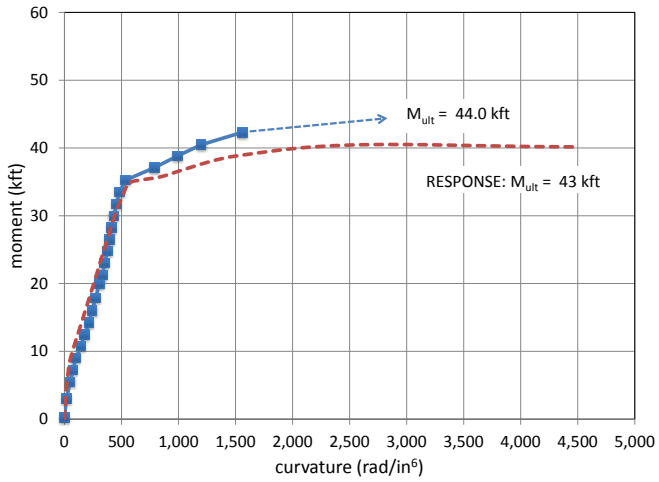

a) Moment-Curvature Plot

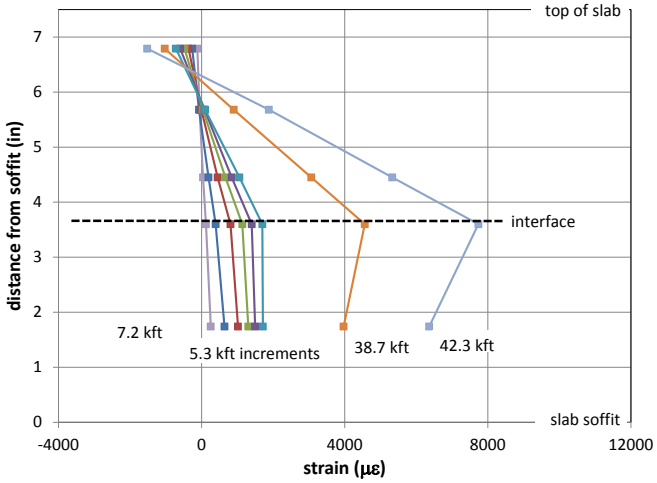

b) Strain Profiles

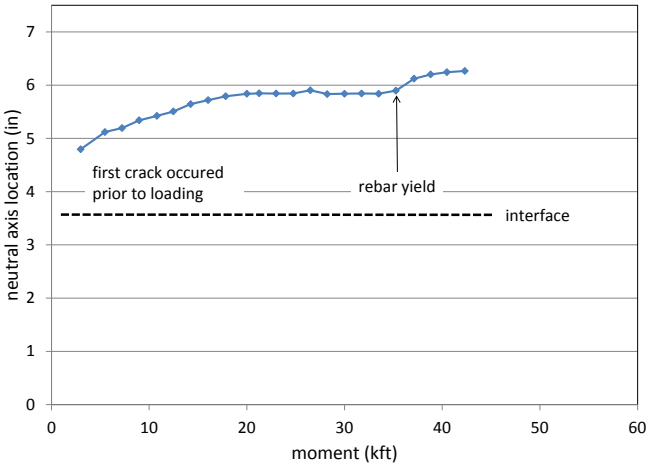

c) Location of Neutral Axis

d) Reinforcement Yield (35.3 kipft)

e) Final DEMEC Reading (42.3 kipft)

f) Ultimate Load (44.0 kipft)

Figure 31: Slab AAA Results

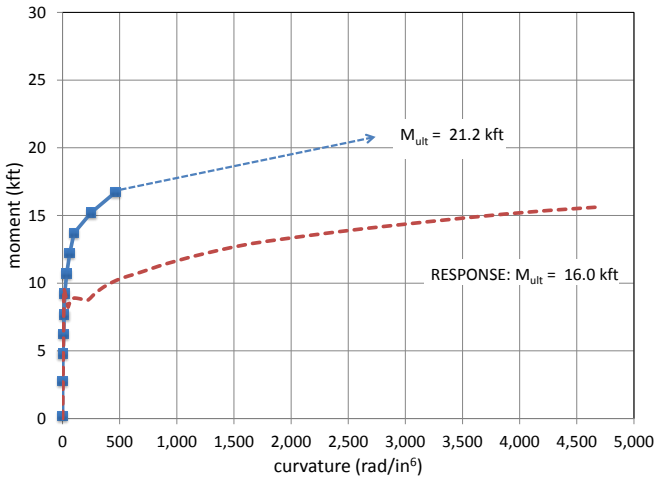

a) Moment-Curvature Plot

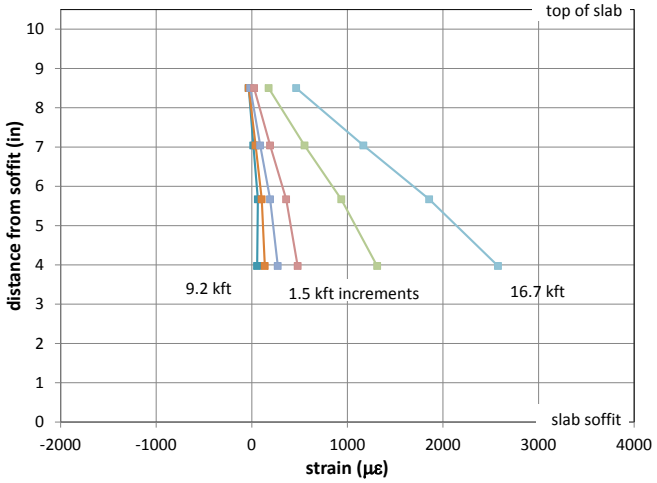

b) Strain Profiles

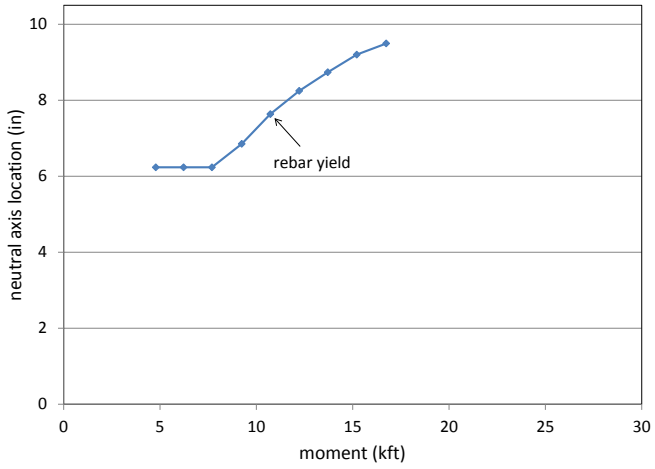

c) Location of Neutral Axis

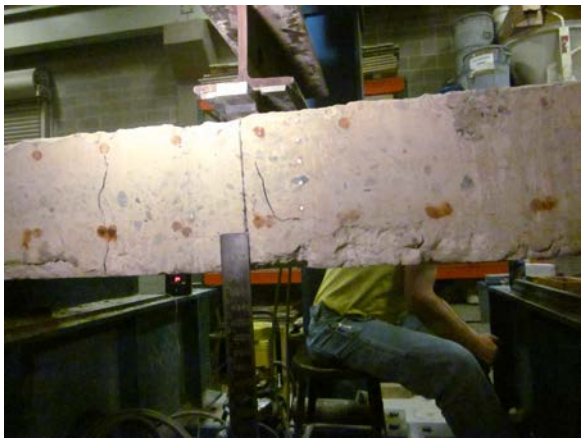

d) Reinforcement Yield (10.7 kipft)

e) Final DEMEC Reading (16.7 kipft)

f) Ultimate Load (21.2 kipft)

Figure 32: Slab M1 Results

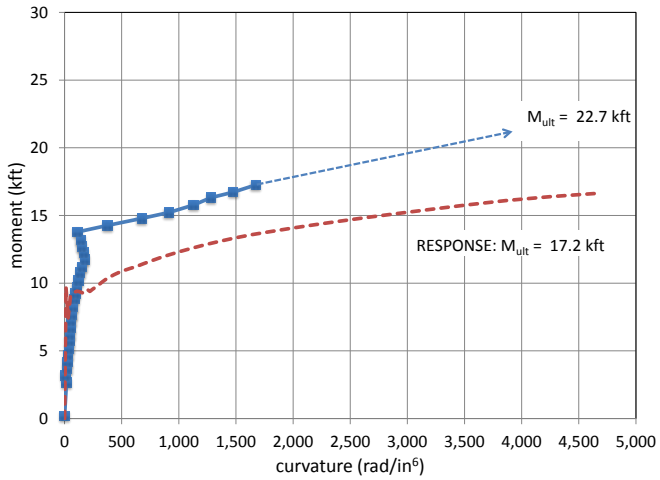

a) Moment-Curvature Plot

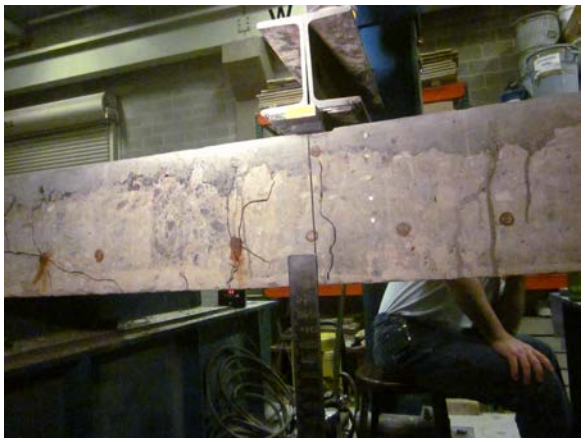

d) Reinforcement Yield (14.3 kipft)

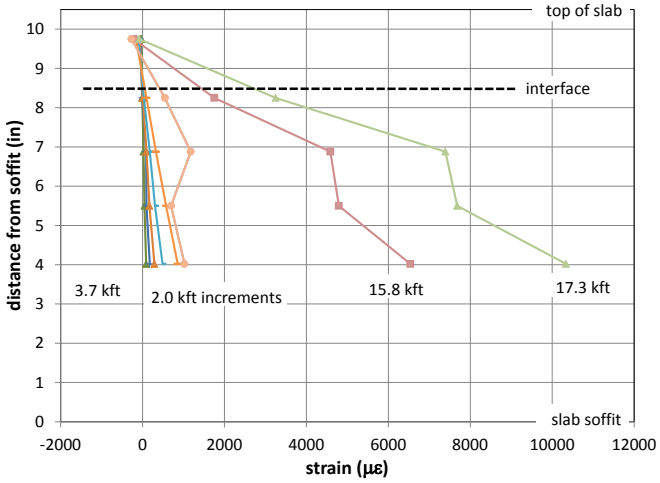

b) Strain Profiles

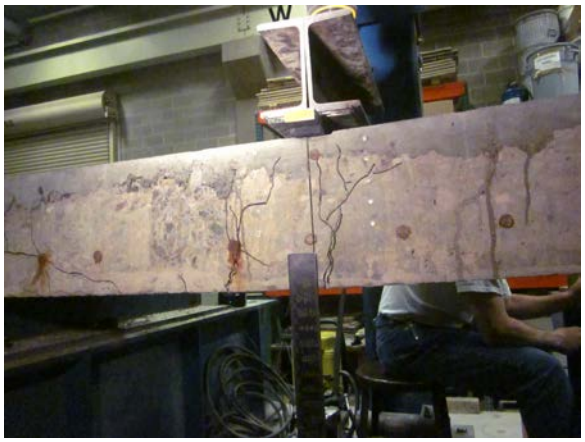

e) Final DEMEC Reading (17.3 kipft)

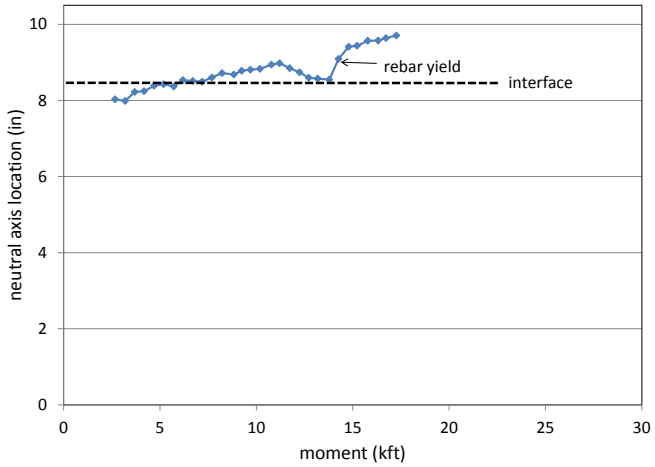

c) Location of Neutral Axis

f) Ultimate Load (22.7 kipft)

Figure 33: Slab M3 Results

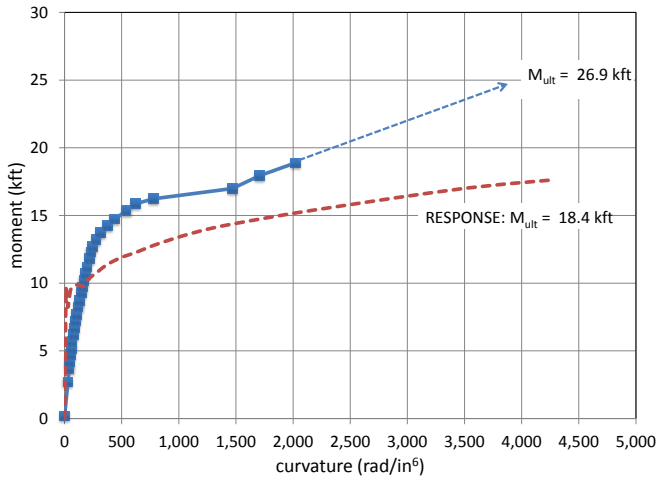

a) Moment-Curvature Plot

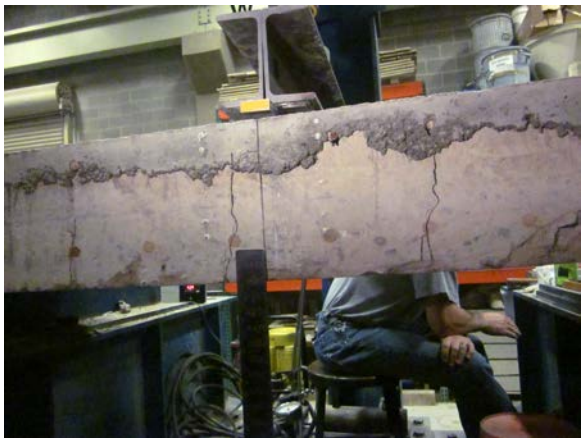

d) Reinforcement Yield (14.3 kipft)

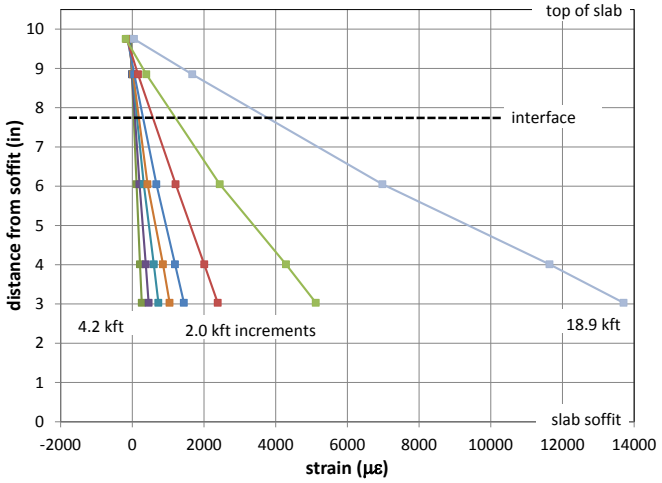

b) Strain Profiles

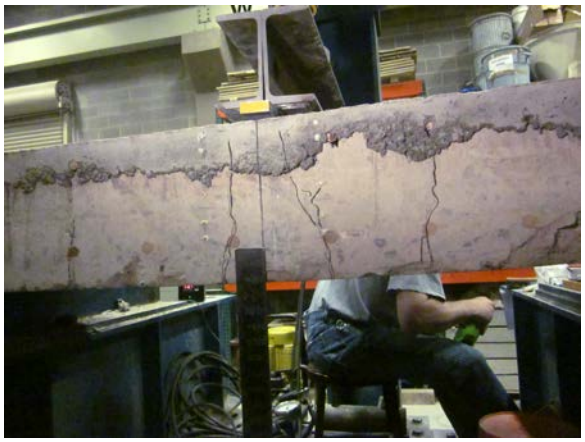

e) Final DEMEC Reading (18.9 kipft)

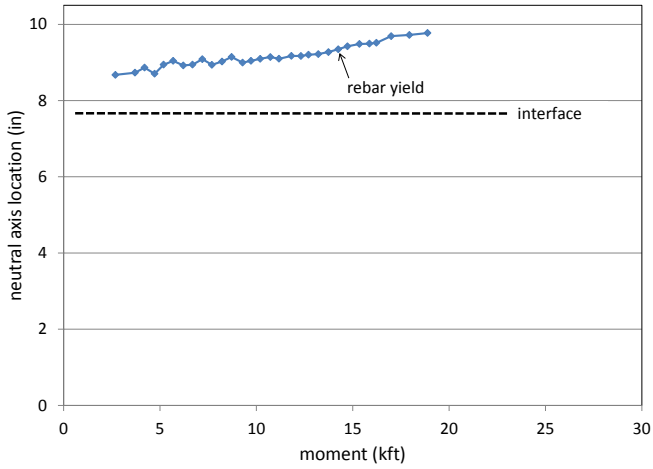

c) Location of Neutral Axis

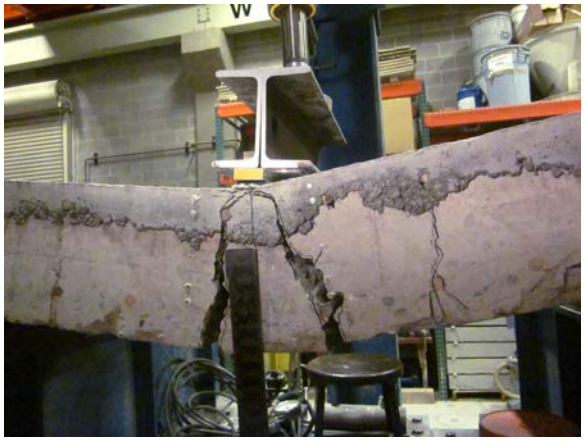

f) Ultimate Load (26.9 kipft)

Figure 34: Slab M4 Results

5.0 DISCUSSION

The following discussion is based on experimental results presented in the previous Chapter. Analytical models as well as material from the literature review are used to supplement the discussion.

5.1 EXPERIMENTAL VS. PREDICTED CAPACITIES

In the course of the experimental program, analytical models (described previously in Section 3.5) were generated for each of the test specimens using RESPONSE. Slab capacities predicted from these plane-sections analyses were generated for the control slab and each tested specimen. Although the laboratory slabs are all under-reinforced (i.e.: behavior governed by reinforcing steel), each analysis considered the actual geometry of the slab, particularly the location of the LMC overlay interface and the different concrete and LMC material properties (Table 5). For instance, the uncracked and cracked moments of inertia will shift slightly because of the small difference in compressive strengths (and therefor moduli) of the substrate and LMC. This affects the sectional response to a small degree.

Figure 35 compares predicted moment capacities for the laboratory specimens generated using RESPONSE, to the experimentally obtained capacities noted in Table 8. Most data falls to the right of the 45 degree line indicating that the experiments uniformly exhibited strengths greater than predicted. This is the ‘desired’ result of this comparison since the analytical model necessarily

makes simplifying assumptions, particularly in terms of material behavior. Two comparisons are presented in Figure 35: a) solid circles and triangles represent comparisons made between experimental and analytical data that reflect the unique geometries of the individual slabs; whereas b) the open data points represent comparisons between experimental data and predictions for Slab A. The latter is more appropriate to design or rating procedures since it considers the 'as-built' capacity of the monolithic slab.

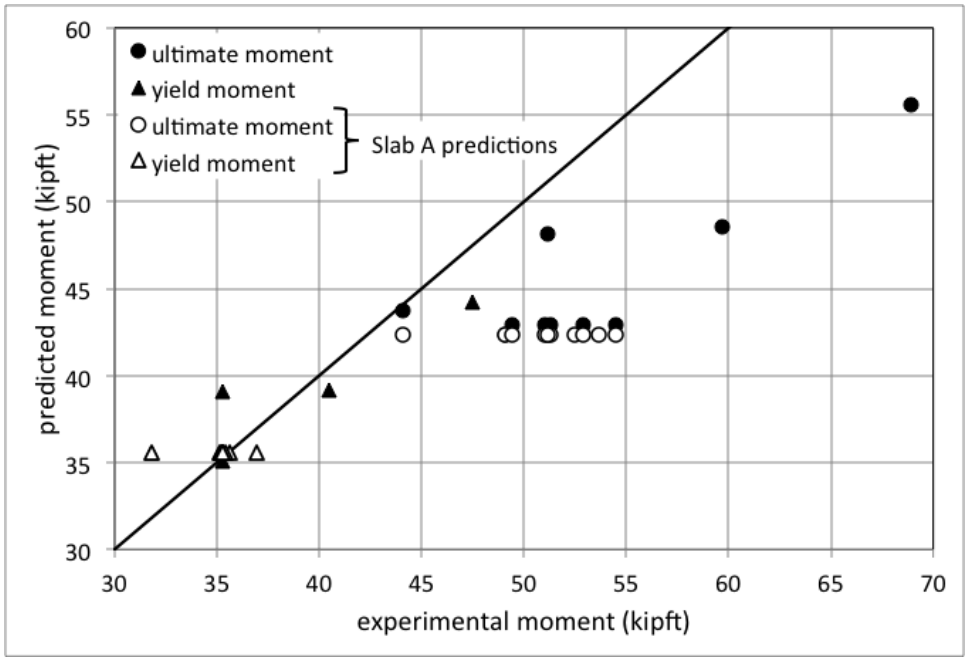

Figure 35: Experimental vs. Predicted Capacities of Laboratory Slabs

Predictions of yield capacity (triangles in Figure 35) were very close, and generally marginally below the experimentally observed values. Since actual reinforcing bar yield strength (f_y = 67.8 ksi (467 MPa)) was used, this good agreement should be expected. Clearly, if nominal material capacities were used (i.e.: f_y = 60 ksi (414 MPa)), the prediction of yield capacity would be that much more conservative. The only slab in which the predicted capacity (39.3 kipft

(53.2kNm)) exceeded the experimentally observed capacity (35.3 kipft (47.9kNm)) was Slab H which was tested in the inverted position with the overlay in the tension region of the cross-section.

Prediction of ultimate slab capacity (circles in Figure 35) and slab failure mode (see Table 8) are similarly uniformly conservative, although not excessively so. The comparison of yield and ultimate capacities validate the use of a simple plane sections analysis (in this case implemented using RESPONSE) for predicting slab capacity regardless of the presence of an overlay.

The Marshall Ave. slabs also outperformed their analytical predictions in every instance as shown in Figure 36 (see also Table 9 and Figures 32-34). Repaired slabs (M3 and M4) exhibited approximately 127% increase in load-carrying capacity at steel yield and 117% increase at ultimate load, when compared to the average comparable values obtained from control specimens M1 and M2. As was the case with the laboratory slabs, the experimentally observed capacities exceeded those predicted for the original as-built slabs (open data points in Figure 36) by a reasonably conservative margin.

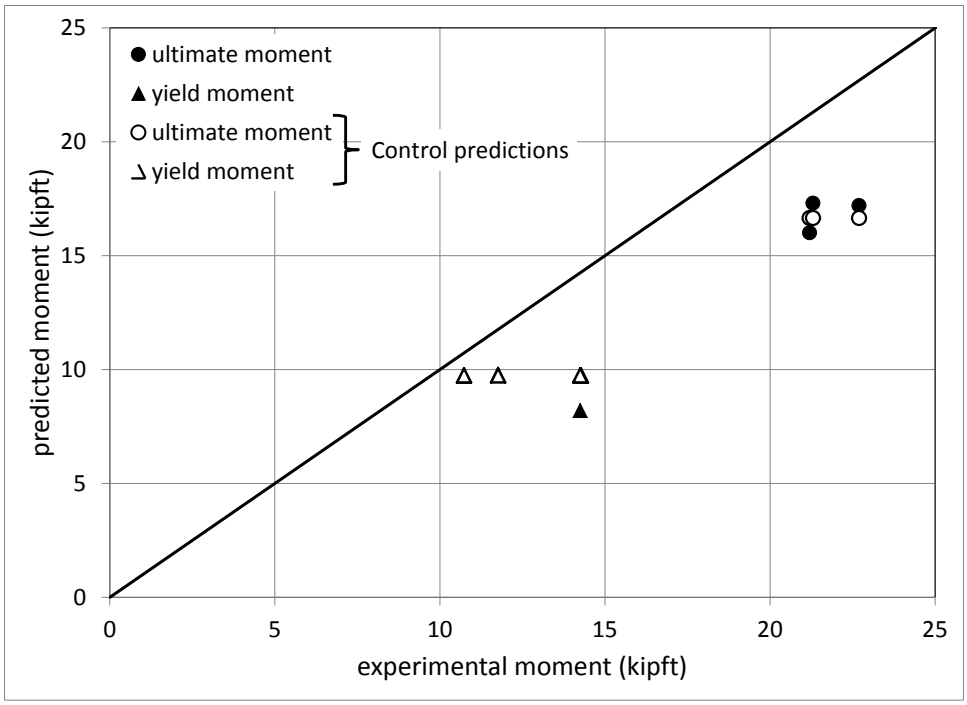

Figure 36: Experimental vs. Predicted Capacities of Marshall Ave. Slabs

Figure 37 shows the entire moment-curvature response of all laboratory slabs (see Figures 22 through 31 for individual curves). Prior to cracking, all slabs with the exception of Slab AAA, exhibit comparable stiffness and cracking loads (see Figure 37b). Slab AAA was unintentionally cracked during removal from the formwork prior to testing therefore no uncracked behavior is present. Nonetheless, the cracked behavior of Slab AAA is comparable to the other slabs. Post-cracking behavior of all slabs was comparable and, as described previously, the yield and ultimate behaviors were all similar.

The deeper Slabs C and B show similar although appropriately stiffer behavior. This is an important observation since not only did the LMC overlayed slabs perform similarly to monolithic slabs, the LMC when used to increase the original slab depth, served to also increase the capacity of the original slab. In this study, Slabs C and B, having depths of 8 and 8.5 in. (203 and 216 mm),

respectively, exhibited yield capacities 1.27 and 1.49 times greater than the 7.5 in. (191 mm) control Slab A. This increase in strength is offset to some extent by the increase in slab self-weight, 1.07 and 1.13 times, respectively. Additionally it must be noted that the self-weight of any *additional* slab thickness must be considered as an imposed load (DW in the AASHTO loading cases) rather than as a dead load (DC) since this additional load does result in stress in the reinforcing steel. Nonetheless, Slabs C and B were effectively strengthened by increasing their depth with the LMC overlay.

Superimposed on Figure 37 is the analytical prediction for Slab A. As is typically seen, the analytical model results in a stiffer behavior than is exhibited experimentally. Once again, this is due to necessary simplification of the analytical model. In this case, the assumption of 'perfect bond' between reinforcing steel and concrete may significantly affect the stiffness in these under-reinforced members.

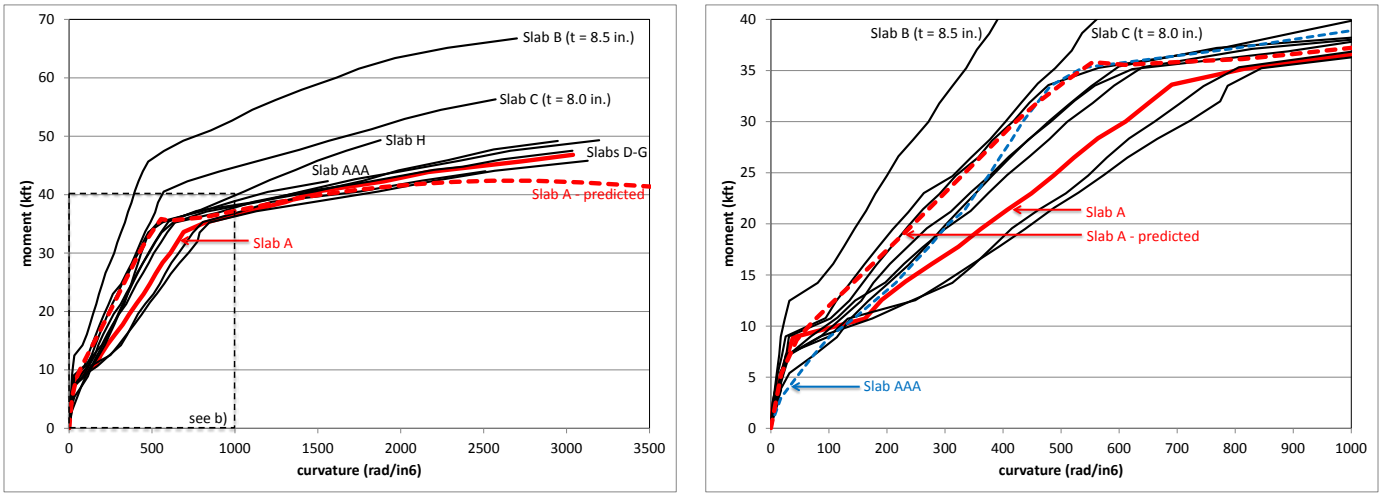

a) Moment-Curvature curves for all slabs

b) detailed Moment-Curvature response showing 'elastic' range.

Figure 37: Moment-Curvature Responses of Laboratory Slabs

Similar trends were observed in the moment curvature responses of the Marshall Ave. slabs. Figure 38 shows the experimentally obtained moment-curvature response of slabs M1

(control, no overlay), M3 and M4. As was the case with the laboratory specimen results, the predicted response was slightly stiffer than the experimental response and the capacity was improved in specimen where overlays were applied. In general, Marshall Ave. slabs tracked well with each other in regards to their moment-curvature behavior. It was expected to have greater scatter and variability among 'field' data than 'laboratory' data, due to a number of unknowns – particularly existing damage – that are present in field specimens. In the case of this experiment such damage may have been caused by the cutting and transportation process as well as the extent of damage that occurred while the slabs were in service.

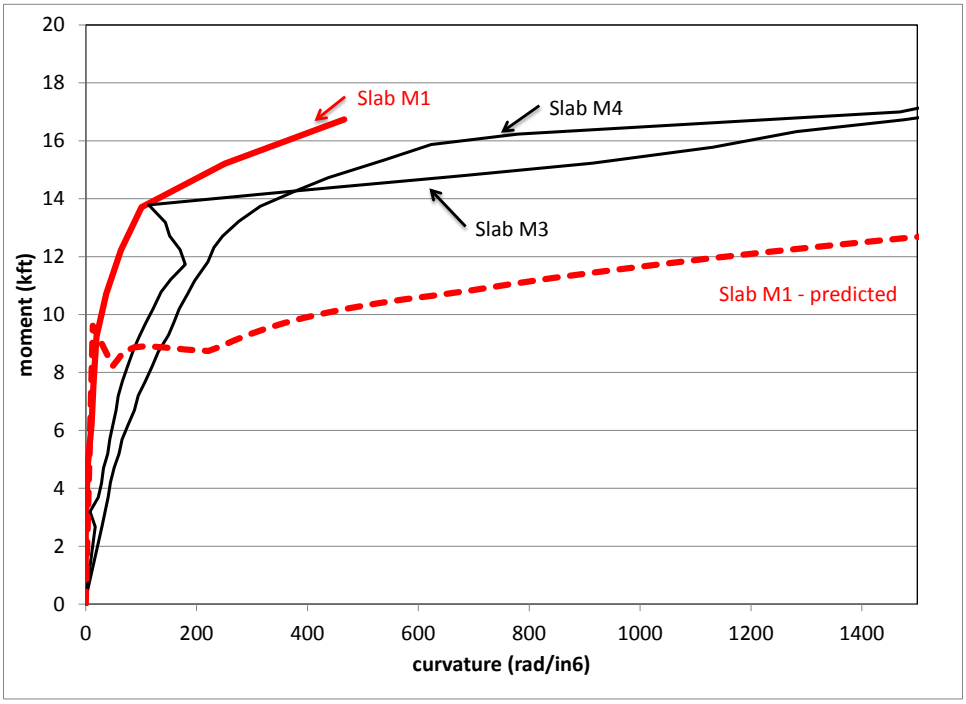

Figure 38: Moment Curvature Reponses of Marshall Ave. Slabs

Figure 39 shows the calculated post-cracking neutral axis depth for all laboratory slabs along with the predicted values for Slab A. Data for individual slabs is provided in Figures 22 through 31. Experimental values tracked each other and the predicted values very well. Once

cracking occurs, the neutral axis shifts upward (theoretically prior to cracking the neutral axis is located at the slab mid depth (3.75 in. (95 mm)) for the laboratory slabs) to a location approximately 5 in. (127 mm) above the soffit. As loading progresses cracking propagates, although since the steel and concrete remain essentially elastic, the neutral axis remains relatively constant as stresses are able to redistribute in the slab section. Yield of the reinforcing steel is evident by an upward 'bump' in the neutral axis (around 35 kipft (47.5 kNm)) and a subsequent continued upward shift as cracking continues to propagate with no further redistribution of stresses in the tension steel possible.

The most important observation in Figure 39 is that there is no obvious effect on the LMC interface. For most slabs, the interface is below the cracked section neutral axis (see Figures 22-31) and above the uncracked neutral axis (approximately 3.75 in. (95 mm) above soffit) and has no obvious effect on slab behavior.

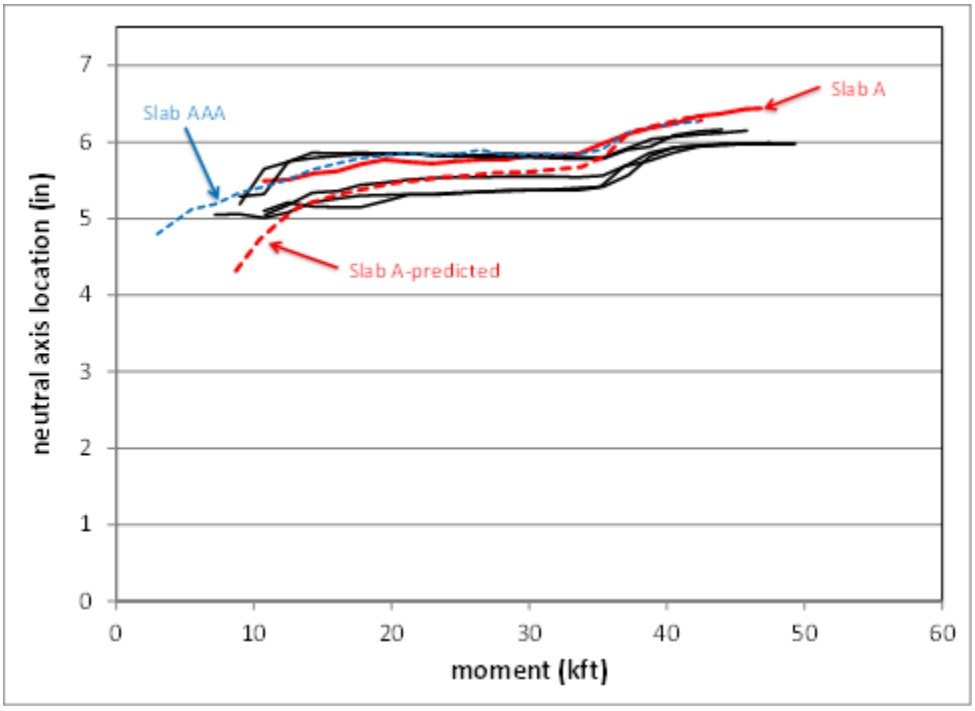

Figure 39: Post-Cracking-Height of Neutral Axis vs. Moment of Laboratory Slabs

Figure 40 shows the height of the neutral axis plotted against the applied moment for the Marshall Ave. slabs also indicating reasonable correlation between experimental and predicted values. Like the laboratory specimens, the height of the neutral axis is observed shifting upward as more load is applied. Since cracking and reinforcing bar yield are essentially simultaneous in these greatly under-reinforced sections (Figure 38) there is no neutral axis 'plateau' evident as in the laboratory slabs.

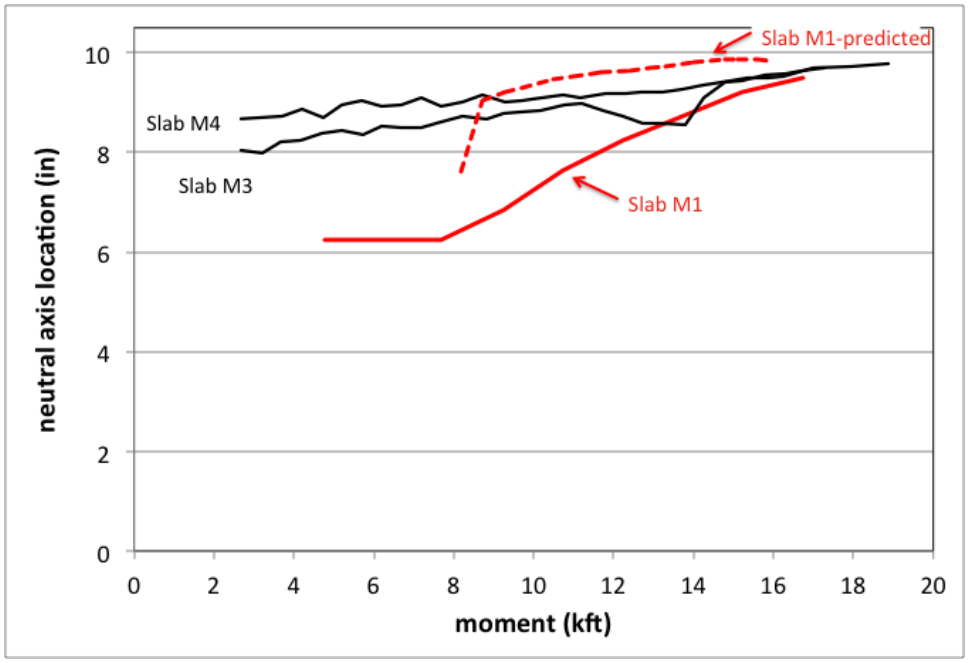

Figure 40: Height of Neutral Axis vs. Moment of Marshall Ave. Slabs

5.2 STRAIN PROFILES

The strain profiles presented in Figures 22-34 did not exhibit any apparent discontinuity associated with the LMC interface. Full composite behavior – no different from that of a

monolithic slab – was observed in all cases. With the exception of when cracking patterns altered strain profiles (see Figure 21), all specimens had a linear strain response through the interface region, indicating no relative movement (slip) between the LMC and concrete substrate.

5.3 CRACK PATTERNS

Composite action was also assessed qualitatively by evaluating crack propagation. Flexural cracks propagated upward from the soffit, through the interface, to the neutral axis. If continuity at the interface was not established, one would expect the cracks to be diverted at the interface (analogous to light refracting in water) rather than remain on the same trajectory. In all parts d and e of Figures 22-34, the cracks are uniformly observed to be unaffected by the presence of the interface.

5.4 STRESSES AT LMC INTERFACE

As discussed earlier, the objective of this study was to establish whether or not composite action was achieved between the substrate and LMC overlay. At the crux of this issue is what magnitude of shear stress is transmitted across the interface. For a homogeneous elastic material, the transverse shear stress is calculated as VAy/It where V = internal shear; A = area of material above interface; y = distance from centroid of A to centroid of gross section; I = moment of inertia of gross section; and, t = width of cross-section at the interface. While this calculation may be valid prior to cracking, it may not be used once the concrete is cracked since A, y and I all vary

and the material may no longer be considered elastic. For cracked concrete, the shear carried across the interface is that required to equilibrate the tension-compression couple developed between the reinforcing steel and compression block concrete. Therefore, for an under-reinforced section controlled by reinforcing steel yield, the maximum value of shear that must be transmitted is $T = A_s f_y$. This is resisted at the section at the top of the tension zone by the area of concrete in the shear span; i.e.; the slab width by half the span (b x L/2). This is shown schematically in Figure 41.

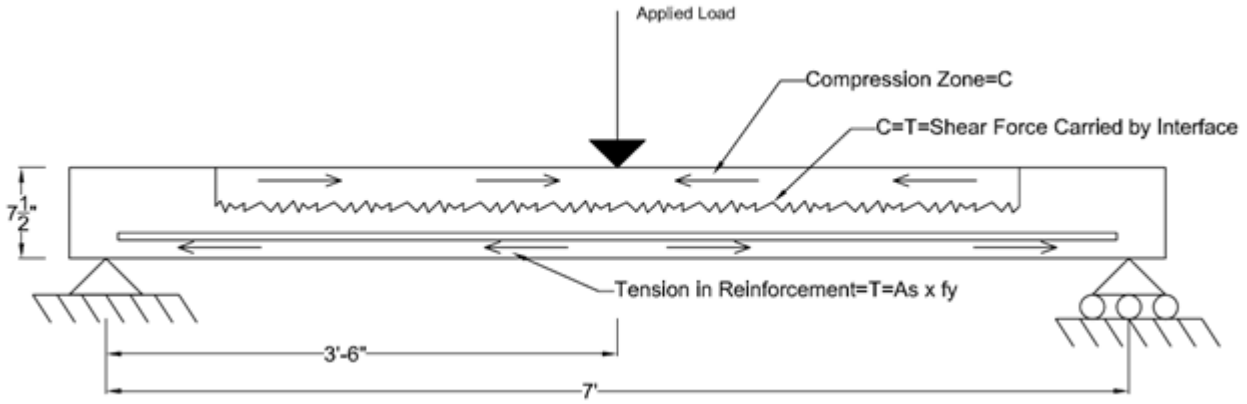

Figure 41: Shear Forces at Interface of Laboratory Slabs

For the laboratory-cast slabs considered in this study, the shear that must be transmitted is developed by the yield of the 4 #5 longitudinal bars:

$$T = A_s f_y = 4(0.31 \text{ in}^2)(67.8 \text{ ksi}) = 84 \text{ kips } (374 \text{ kN})$$

This is resisted over the horizontal area of the concrete in the shear span:

$$A_c = b(L/2) = 22 \text{ in. x } 84 \text{ in.}/2 = 924 \text{ in}^2 \ (5.96 \text{ x } 10^5 \text{ mm}^2)$$

Resulting in an interfacial shear stress of 84 kips/924 in^2 = 91 psi. (0.63 MPa).

The concrete shear resistance along a match cast interface was discussed in Section 1.2.2 and a number of values given in Table 1. For the LMC interfaces in this study, the 'implied aggregate interlock capacity' (Table 1) ranges from 240 psi (1.66 MPa) (AASHTO 2010) to 390 psi (2.69 MPa) (Harries et al. 2012). Similarly, suggested minimum interface tension strengths

range from 100 psi (0.689 MPa) (Wenzlick 2002) to 200 psi (1.38 MPa) (Basham 2004), where these values are considered to be at most one half of the shear capacity (Silfwerbrand 2009). A companion study (to be reported by subsequently by M. Sweriduk) conducted pull-off tests on all slabs reported in this study. The average pull-off strength achieved for the laboratory slabs having LMC exceeded 300 psi (2.07 MPa) and the direct tension capacity of Slab A was found to be 373 psi (2.58 MPa). Therefore, by any measure, the shear stress required to yield the reinforcing steel in the laboratory slabs (91 psi (0.63 MPa)) is considerably less than the anticipated (or indirectly measured) capacity of the interface.

Considering the AASHTO-implied lowest value of interface shear resistance, 240 psi (1.66 MPa), the slab longitudinal tensile reinforcement ratio, $\rho = A_s/hb$ would have to be increased from the existing value of 0.0075 to almost 0.02 before interface stresses approached the implied capacity. Such a heavily reinforced slab (equivalent to #5 bars at 2 in. or approximately #8 bars at 5.5 in. in a 7.5 in deep slab) is unlikely for a bridge deck. Nonetheless, this line of enquiry does identify older heavily reinforced ‘slab bridges’ having no shear reinforcement as poor candidates for overlay repair since the interface stresses may be higher.

5.5 EFFECT OF VARYING CONCRETE AND LMC STRENGTHS

Good practice dictates that the LMC overlay should be designed to closely match the material properties of the substrate concrete (Silfwerbrand 2009). For the laboratory slabs reported in this study, the compressive strengths at the time of testing of the LMC and substrate concrete

differed by less than 100 psi (0.69 MPa) – less than 1.5% of the compressive strength (Table 6). The Marshall Ave. slabs provided a greater difference of approximately 1500 psi (10.3 MPa).

Using the same RESPONSE model presented previously, a parametric study was conducted in which all parameters but LMC and substrate concrete strength were maintained constant. The model was generated using the cross-sectional geometry of the laboratory slabs with the LMC interface located at the slab mid depth (3.75 in. (95 mm)) thereby ensuring the LMC constituted the entire compression zone even prior to cracking. The LMC and substrate concrete strengths were combined in every combination from 3000 to 8000 psi in 1000 psi increments (20.7 to 55.2 MPa in 6.9 MPa increments).

As should be expected for under-reinforced slabs, varying the concrete strength between the overlay and substrate had very little effect on yield or ultimate capacity. Yield moments varied by a maximum of only 3% and ultimate moments by 7%, for all combinations tested. Ultimate moments were improved as substrate concrete strength was increased, but exhibited no similar trend as a result of the increase of overlay strength. This result reflects the under-reinforced nature of the slabs being governed by the steel tension response and the fact that the effects of tension-stiffening were included in the model (Bentz 2000). The results of the analytical model are also supported by the experimental results of the Marshall Ave. slabs, where altering LMC and substrate compressive strengths had no noticeable detrimental effects on slab behavior.

6.0 CONCLUSIONS

The main objective of this study was to assess the validity of *PennDOT Publication 15 Section 5.5.5.1*, specifically that "a latex overlay is not considered structurally effective", in terms of the structural response of the bridge superstructure. Experimental evidence from this study clearly demonstrates that the LMC overlay is structurally effective in terms of load carrying capacity. Several parameters were varied amongst test specimens in the experimental program: overlay depth, removal of concrete 'shadows' under primary reinforcement bars, and the direction of bending (positive and negative moments). The LMC-repaired slabs acted as monolithic slabs in all cases – laboratory slabs and decommissioned Marshall Ave. slabs – and the capacity was uniform regardless of LMC depth. The capacity of the LMC-repaired slabs exceeded their predicted ultimate capacities in all cases. Additionally, the LMC-repaired slab capacity exceeded the ultimate capacity of the control slab in all cases. Finally, it was demonstrated based on fundamental mechanics and shear friction theory that LMC interface stresses are relatively low and unlikely to exceed reasonable values of capacity for properly constructed LMC overlay repairs. Therefore it is recommended that the statement made in *PennDOT Publication 15 Section 5.5.5.1* be amended to the following; "latex overlay shall be considered structurally effective, provided the overlay is deeper than 1.25 inches."

This proposed revision is made with the recommendation that several other parameters be followed in order to insure a quality LMC overlay repair:

- Best construction practices, described at length in the literature review, are followed. Briefly these include:

- Attention should be given to the surface condition of interface before placement of the overlay. This includes proper moisture conditioning and cleaning all debris and laitance from the interface. Cleanliness of the interface was mentioned in numerous works as being one of the more critical issues that control overlay performance.
- Although no effect of having concrete 'shadows' below the bars were observed in Slab F*, it is nonetheless recommended that all shadows, were they occur, be removed.
- Like all concrete construction care should be taken in the placement process to avoid segregation. At the same time compaction should allow for all air voids to be filled without causing segregation.
- LMC overlays should be allowed to cure for the appropriate length of time and under the recommended conditions.
- Available literature and anecdotal evidence suggests that hydrodemolition is the preferred method of concrete removal, although alternative methods of concrete removal (pneumatic hammers) were not assessed in this study.

- A pull-off testing program, based in ASTM 1583, for quality assurance is established for LMC overlay projects.

A number of additional conclusions were drawn from this study:

The anticipated capacity of an LMC overlayed deck may be estimated as that of the original full-depth deck. Experimental capacities were seen to exceed this value in all cases. Simple plane sections analyses of either the original full-depth deck or LMC-repaired deck are suitable for obtaining these capacities.

The LMC interface has essentially no effect on the behavior of the repaired slabs. No evidence of 'buckling' or slip failure was observed (see Figure 3). No evidence of the interface affecting crack propagation was observed.

The interface shear capacity is expected to exceed the demand for bridge slabs typical of slab-on-girder bridges. Nonetheless, older heavily reinforced 'slab bridges' having no shear reinforcement are believed to be poor candidates for overlay repair since the interface stresses will be higher.

This study has demonstrated the effectiveness of PennDOT Method 2 LMC overlays for Type 1 and 2 bridge deck repairs. The LMC clearly contributes to the load carrying capacity of the rehabilitated deck slab. With this conclusion, it is envisioned that more bridges that would otherwise be subject to complete deck replacement may be viable candidates for overlay repair. This, it is believed, will conserve resources directed to an individual bridge and significantly speed the deck rehabilitation process.

6.1 RECOMMENDATIONS FOR FURTHER RESEARCH

The following are areas require further research in order to improve the understanding of the structural response of LMC overlays:

- Further tests of slabs having very thin overlays are warranted. The observations of the present study indicate that 'buckling' of the overlay (as shown in Figure 3) is not likely however previous research (Cole et al. 2002) has identified this failure mode.

- Few studies have addressed the response of LMC overlays subject to realistic fatigue loads. Fatigue testing of slab flexural specimens would mimic more closely the in-situ forces of the overlay repair. In particular, the question of fatigue-induced deterioration of the interface shear resisting capacity remains unanswered.
- The effect of variation between LMC and substrate concrete thermal expansion coefficients was not assessed during the course of this study. Variation of thermal expansion coefficients could induce stresses at the interface, due to differential movement. Further tests evaluating the magnitude of these stresses under in-situ temperature cycles would reveal if this variation is harmful to the overlay system's performance.
- Although hydrodemolition is recommended in this and other studies, comparable tests on slabs having different demolition methods are warranted. Such tests would require quantification of the damage to the substrate concrete resulting from the demolition process. Hydrodemolition is expensive and impractical in some cases, permitting mechanical demolition and understanding its effect on performance increases the potential application for LMC overlays.
- Specific study of the economic (life cycle cost assessment) and environmental (life cycle assessment) of bridge deck overlay versus bridge deck replacement is necessary. Based on the current study, and those available in the literature, there is little evidence to suggest extending the expected life of an LMC overlay beyond the presently anticipated 20 years. There is, however, little evidence suggesting that a service life beyond 20 years is not feasible.

BIBLIOGRAPHY

ACI Committee 318 (2011). *Building Code Requirements for Structural Concrete (ACI318-11) and Commentary (ACI 318R-11)*. Farmington Hills, MI: American Concrete Institute.

ACI Committee 546 (2004) *Concrete Repair Guide*. Farmington Hills, MI: American Concrete Institute.

Alhassan, M. A. and Issa, M. A. (2010) "Long-term Protection of Bridge-deck Systems with Structural Latex-Modified Concrete Overlays." *PCI Journal*, 122-137.

American Association of State Highway and Transportation Officials (AASHTO) (2010). *AASHTO LRFD Bridge Design Specifications*, 5th edtion.

American Society for Testing and Materials (ASTM) (2013). *C1583-13 Standard Test Method for Tensile Strength of Concrete Surfaces and the Bond Strength or Tensile Strength of Concrete Repair and Overlay Materials by Direct Tension (Pull-off Method)*. ASTM, West Conshohocken, PA.

ASTM International (2012) *C39 Standard Test Method for Compressive Strength of Cylindrical Concrete Specimens*, West Conshohocken, PA. 7 pp.

ASTM International (2013) *C42 Standard Test Method for Obtaining and Testing Drilled Cores and Sawed Beams of Concrete*, West Conshohocken, PA. 7 pp.

ASTM International (2010) *C78 Standard Test Method for Flexural Strength of Concrete (Using Simple Beam with Third-Point Loading)* West Conshohocken, PA. 4 pp.

ASTM International (2011) *C496 Standard Test Method for Splitting Tensile Strength of Cylindrical Concrete Specimens*, West Conshohocken, PA. 5 pp.

ASTM International (2012) *D4580-03 Standard Practice for Measuring Delaminations in Concrete Bridge Decks by Sounding*. West Conshohocken, PA. 4 pp.

Bartlett, F.M. and MacGregor, J.G. (1994) "Effect of Core Diameter on Concrete Core Strengths." *ACI Materials Journal*, 91(5), pp. 460-470.

Basham, K. (2004) *Testing and Evaluation of Concrete Repair Materials for the Cheyenne Airport Taxiways*. Cheyenne: State of Wyoming Department of Transportation; U.S. Department of Transportation.

Bentz, E.C. (2000) *Sectional Analysis of Reinforced Concrete Members-PhD Thesis*, Department of Civil Engineering, University of Toronto, pp. 310.

Birkeland, P.W., and Birkland, H.W. (1966) "Connections in Precast Concrete Construction." *Journal of the American Concrete Institute*, 63(3), 345-368.

Cole, J., Shahrooz, B. M. and Gillum, A. J. (2002) "Performance of Overlays under Static and Fatigue Loading." *ASCE Journal of Bridge Engineering*, 7(4), 206-213.

Eveslage, T., Aidoo, J., Harries, K. A. and Bro, W. (2010) "Effect of Variations in Practice of ASTM D7522 Standard Pull-Off Test for FRP-Concrete Interfaces." *ASTM Journal of Testing and Evaluation*, 38(4), 424-430.

Federal Highway Administration (FHWA) (2011) *Deck Structure Type*, http://www.fhwa.dot.gov/bridge/nbi/deck.cfm, Retrieved October 24, 2012.

Fowler, D., and Trevino, M. (2011) Overlay Design Process, *Bonded Cement-Based Material Overlays for the Repair, the Lining or the Strengthening of Slabs or Pavements*, RILEM State-of-the-Art Report, Vol. 3, 5-16.

Germann Instruments, Inc. (2012) *Bond-Test*, Evanston, IL.

Gillum, A. J., Cole, J., Turer, A. and Shahrooz, B. M. (1998) *Bond Characteristics of Overlays Place Over Bridge Decks Sealed with HMWM or Epoxy*, University of Cincinnati, College of Engineering. Cincinnati Infrastructure Institute.

Gillum, A. J., Shahrooz, B. M. and Cole, J. (2001) Bond Strength Between Sealed Bridge Decks and Concrete Overlays. *ACI Structural Journal*, 98(6), 872-879.

Harries, K.A., Kasan, J. and Aktas, C. (2009) *Repair Methods for Prestressed Concrete Bridges*, Report No. FHWA-PA-2009-008-PIT 006. 170 pp.

Harries, K.A., Zeno, G. and Shahrooz, B.M., (2012) "Toward an Improved Understanding of Shear Friction Behavior." *ACI Structural Journal*, 109(6), pp 835-844.

International Concrete Repair Institute (ICRI) (2004). *Guideline No. 03739 Guide to Using In-Situ Tensile Pull-Off Tests to Evaluate Bond of Concrete Surface Materials*, ICRI, Des Plaines, IL.

Kahn, L. F., and A. D. Mitchell (2002). "Shear Friction Tests with High Strength Concrete." *ACI Structural Journal*, 99 (1), 98-103.

PennDOT *Publication 15: Design Manual Part 4: Structures*, May 2012. accessed via: ftp.dot.state.pa.us/public/PubsForms/Publications/PUB 15M.pdf

PennDOT *Publication 408: Construction Specifications*, April 2011. accessed via: ftp.dot.state.pa.us/public/bureaus/design/pub408/pub 408-2011.pdf

RILEM (2011) *Bonded Cement-Based Material Overlays for the Repair, the Lining or the Strengthening of Slabs or Pavements*, State-of-the-Art Report of the RILEM Technical Committee 193-RLS, Bissonnette, B., Courard, L., Fowler, D.W. and Granju, J.-L. (editors)/ RILEM State-of-the-Art Reports, Vol. 3. Reunion Internationale des Laboratoires et Experts des Materiaux, Systemes de Construction et Ouvrages, Bagneux, France.

Shahrooz, B. M., Gillum, A. J., Cole, J. and Turer, A. (2000) "Bond Characteristics of Overlays Placed Over Bridge Decks Sealed with HMWM." *Transportation Research Record*, 1697, 24-30.

Silfwerbrand, J. (2009) "Bonded Concrete Overlays for Repairing Concrete Structures." *Failure, Distress and Repair of Concrete Structures*, Woodhead Publishing Limited, Oxford UK, 208-243.

Silfwerbrand, J., Beushausen, H. and Courard, L. (2011) Bond, *Bonded Cement-Based Material Overlays for the Repair, the Lining or the Strengthening of Slabs or Pavements*, RILEM State-of-the-Art Report, Vol. 3, 59-79.

Vaysburd, A. M. and McDonald, J. E. (1999) *An Evaluation of Equipment and Procedures for Tensile Bond Testing of Concrete Repairs*, US Army Corp of Engineers, Washington, DC.

Vaysburd, M. and Bissonnette, B. M. (2011) "Practice and Quality Assurance." *Bonded Cement-Based Material Overlays for the Repair, the Lining or the Strengthening of Slabs or Pavements*, RILEM State-of-the-Art Report, Vo. 3, 157-170.

Wenzlick, J. D. (2002) *Hydrodemolition and Repair of Bridge Decks*, Missouri Department of Transportation, Research, Development and Technology. Jefferson City, MO.

Zeno, G.A. (2009). *Use of High-Strength Steel Reinforcement in Shear Friction Applications-Master's Thesis.* University of Pittsburgh, Swanson School of Engineering. Watkins-Haggart Structural Engineering Laboratory.